Bull Volcanol (1991) 54:25-49

Bulletin of
Volcanology

The 1976–1982 Strombolian and phreatomagmatic eruptions of White Island, New Zealand: eruptive and depositional mechanisms at a 'wet' volcano

BF Houghton and IA Nairn

DSIR Geology and Geophysics, PO Box 499, Rotorua, New Zealand

Received December 3, 1991

Abstract. White Island is an active andesitic-dacitic composite volcano surrounded by sea, yet isolated from sea water by chemically sealed zones that confine a long-lived acidic hydrothermal system, within a thick sequence of fine-grained volcaniclastic sediment and ash. The rise of at least 10^6 m^3 of basic andesite magma to shallow levels and its interaction with the hydrothermal system resulted in the longest historical eruption sequence at White Island in 1976–1982. About 10^7 m^3 of mixed lithic and juvenile ejecta was erupted, accompanied by collapse to form two coalescing maar-like craters. Vent position within the craters changed 5 times during the eruption, but the vents were repeatedly re-established along a line linking pre-1976 vents. The eruption sequence consisted of seven alternating phases of phreatomagmatic and Strombolian volcanism. Strombolian eruptions were preceded and followed by mildly explosive degassing and production of incandescent, blocky juvenile ash from the margins of the magma body. Phreatomagmatic phases contained two styles of activity: (a) near-continuous emission of gas and ash and (b) discrete explosions followed by prolonged quiescence. The near-continuous activity resulted from streaming of magmatic volatiles and phreatic steam through open conduits, frittering juvenile shards from the margins of the magma and eroding loose lithic particles from the unconsolidated wall rock. The larger discrete explosions produced ballistic block aprons, downwind lobes of fall tephra, and cohesive 'wet' surge deposits confined to the main crater. The key features of the larger explosions were their shallow focus, random occurrence and lack of precursors, and the thermal heterogeneity of the ejecta. This White Island eruption was unusual because of the low discharge rate of magma over an extended time period and because of the influence of a unique physical and hydrological setting. The low rate of magma rise led to very effective separation of magmatic volatiles and high fluxes of magmatic gas even during phreatic phases of the eruption. While true Strombolian phases did occur, more frequently the decoupled magmatic gas rose to interact with the conduit walls and hydrothermal system, producing phreatomagmatic eruptions. The form of these 'wet' explosions was governed by a delicate balance between erosion and collapse of the weak conduit walls. If the walls were relatively stable, fine ash was slowly eroded and erupted in weak, near-continuous phreatomagmatic events. When the walls were unstable, wall collapse triggered larger discrete phreatomagmatic explosions.

Introduction

White Island, at the northeastern extremity of Taupo Volcanic Zone in New Zealand, is an unusual composite volcano in that its active subaerial vent is located below sea level (Figs. 1, 2). An abundance of shallow, but nonmarine groundwater has played a critical role during observed eruptions. The volcano has a history of frequent small phreatic and phreatomagmatic eruptions, interrupting long intervals of continuous intense, fumarolic and hydrothermal activity (Cole and Nairn 1975). Both styles of activity reflect this unusual hydrologic setting (Houghton and Nairn 1989a–c). Crater-forming eruptions occurred in 1933, 1947, 1965–1966, 1968, 1971, 1976–1982, and 1986–1991. The 1976–1982 eruption sequence was the longest and largest historical event (Table 1), triggered by the rise of at least 10^6 m^3 of basic andesitic magma to shallow levels. The sequence was studied using geological, geophysical, and chemical techniques described by several authors in Houghton and Nairn (1989a).

Setting

White Island is the elliptical top of a 700-m-high submarine andesite-dacite composite volcano with a 17-km basal diameter. The island consists of two overlapping composite cones, an older eroded western cone, and the younger central cone that forms most of the island (Black 1970; Duncan 1970). A 0.5 km by 1.25 km crater

Fig. 1. Aerial view of White Island from the east in June 1982. Steam plume rises from vents within of 1978 Crater Complex at the western end of the main cater floor. Photograph courtesy D. L. Homer

('main crater'), which occupies the eastern and central portions of the island, is breached on its southeastern side (Fig. 1). The main crater has a volume of about 0.2 km^3 and is subdivided into three subcraters (Fig. 2) by spurs projecting inwards from the crater walls (Nairn and Houghton 1989). Vents that have been active in historical times are confined to the western subcrater and the western half of the central subcrater. The subcraters are infilled with unconsolidated, fine-grained, volcaniclastic sediments and tephra, saturated with hot brine acidified by dissolved volcanic gases. Numerous fumaroles and hot springs discharge on the floor of the main crater, forming the subaerial expression of a long-lived acidic hydrothermal system related to the deeper magmatic system of the volcano (Giggenbach and Sheppard 1989). The hydrothermal discharges show no isotopic evidence for sea water in the system (Giggenbach 1987), probably because of chemical sealing of the margins of the hydrothermal system (Houghton and Nairn 1989c). However, the impermeable zones that exclude sea water also confine fumarolic condensates and meteoric groundwater beneath the main crater, saturating this region with the acidic brine that causes rapid rock alteration.

The floor of the main crater is covered by a debris avalanche deposit, with conspicuous hummocky topography (Fig. 1), which formed by crater wall collapse in September 1914, blocking a long-established vent system in the western subcrater. Subsequent activity until 1976 consisted of a succession of small (10^4–10^5 m^3 DRE) phreatic and phreatomagmatic eruptions through the debris avalanche deposits, forming a series of maar-like collapse craters, 50–200 m wide (Fig. 2).

Precursory activity

Widespread uplift of the floor of the main crater of White Island began in mid-1973, reaching its peak in late 1976 or early 1977 (i.e. during the first of the three cycles of the eruption). From mid-1977 until 1984 widespread deflation was recorded, even during Strombolian phases (Clark and Otway 1989). Two small areas on the crater floor underwent more localised and intense

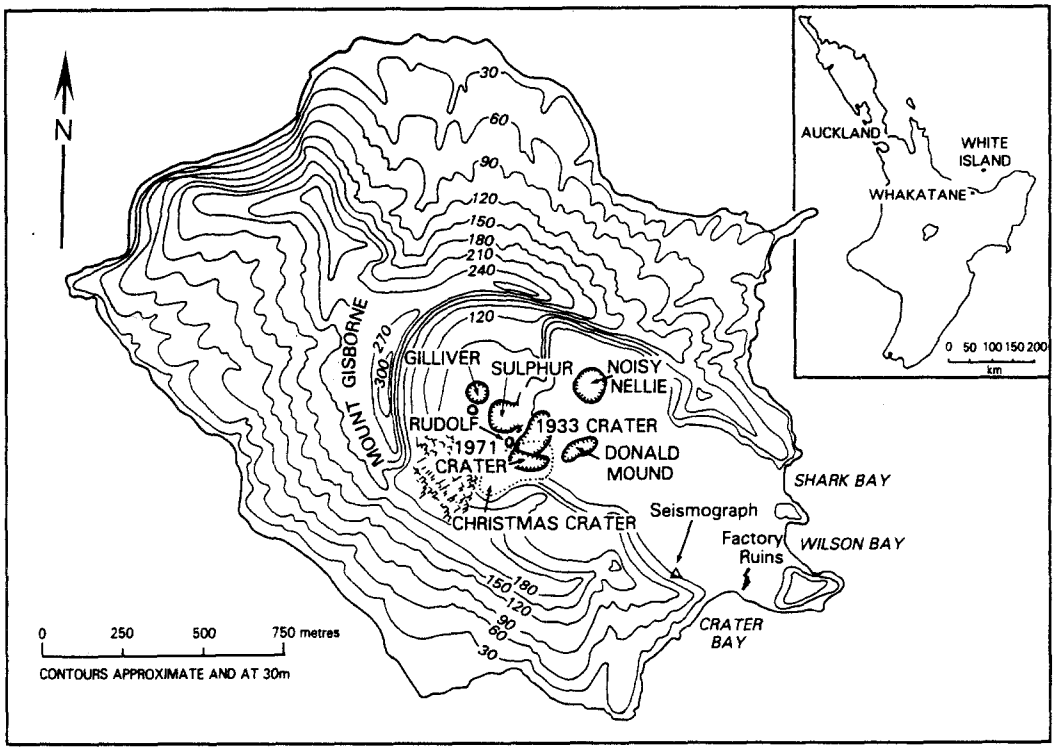

Fig. 2. Location map for White Island volcano showing positions of collapse craters and vents formed prior to December 1976. A dotted line shows the outline of Christmas Crater, formed in 1976–1977

Table 1. Summary of key features and significant events in the 1976–1982 eruption sequence at White Island

Duration	62 months
Tephra volume	10^7 m^3
Magma volume	10^6 m^3
Magma	Basic andesite (55–57% SiO_2)
Style	Phreatic:phreatomagmatic:Strombolian
Chronology:	
June 1973	Onset of widesprad inflation
18 December 1976	Initial phreatomagmatic eruptions
December 1976–February 1977	Slow formation of first collapse crater
March 1977	First and largest Strombolian phase
March 1977	Peak of inflation
March 1978	Largest phreatomagmatic eruptions
March 1978	Rapid collapse of second crater
July 1978	Amalgamation of collapse craters
January 1982	Final phreatomagmatic events

deformation. The vent region had begun rising in 1972, with a dramatic increase in the rate of inflation from early 1976 until destruction of the survey pegs in early 1977. The Donald Mound area, 200–300 m to the east (Fig. 2), showed more complex behaviour, with small peaks of inflation in early 1975, May 1980, and October 1982, and a major peak in March 1978. Hot fumaroles on Donald Mound showed 200–400° C increases in temperature at the time of the peaks in localised inflation at this site (Giggenbach and Sheppard 1989). A significant decrease of the total magnetic field strength beneath the main crater, which occurred between June 1973 and mid-1977, is consistent with heating at a depth of 600–800 m (Christoffel 1989). A general increase in magnetic intensity after November 1982 indicated cooling at depth. The significance of this data is discussed in the interpretation section.

The eruption sequence

The 1976–1982 eruptive sequence contained seven phases of alternating phreatomagmatic and Strombolian volcanism (Tables 1, 2). The alternations of phases (Fig. 3) define three generalised cycles of activity (Houghton et al. 1983). As it is not possible to present every detail of the 5 years of eruption here, we present a brief summary and then descriptions of well-recorded, representative intervals of eruption. A detailed account of the entire eruptive sequence is given in Houghton and Nairn (1989b).

A total of ca. 10^7 m^3 of mostly ash-sized, mixed lithic and juvenile ejecta was erupted in 1976–1982, but the formation of two collapse craters, Christmas and Gibrus craters, strongly modified the near-vent topography, so that no well-defined tuff ring or cone formed. Instead, much of the western subcrater was engulfed by the new collapse craters, and only a small apron of pyroclastic fall and surge deposits formed on the main crater floor, east of the collapse craters. These deposits were rapidly channelled by erosion while more distal ash deposited on the steep inner and outer walls of the main crater was quickly removed by runoff and slope processes.

The first phreatomagmatic phase (P1) lasted 40 days and consisted of weakly explosive, near-continuous emission of gas and ash to form low, poorly sustained convective plumes (Fig. 4a). It produced a laminated fall deposit of volume 10^5–10^6 m^3. The first Strombolian phase (S1) lasted 90 days, although most of the deposits accumulated over a time interval as short as 15 days. It produced a andesitic lapilli and bomb deposit of volume 5×10^5 m^3 over most of the eastern end of the island. The P2 phase lasted 70 days with an initial period of several small, discrete phreatomagmatic explosions, followed by a longer interval of near-contin-

Table 2. Chronology of the 1976–1982 eruption sequence at White Island volcano, New Zealand

Date	Phase duration (days)		Description	Source vent (see Fig. 4)	Comments
18. 12. 76–25. 1. 77	P1	40	Formation of Christmas Crater; near-continuous phreatomagmatic emission of ash in columns to 1 km; emission velocities <50 m/s	1	Erupted material stripped from the conduit by gas and vapour in advance of magma; progressive collapse of crater
2. 77–11. 3. 77		40	Episodic eruption of nonvesicular juvenile ash and minor lithic ejecta, including blocks	1	Eruption of material from cooled margins of advancing magma column during mild degassing of column interior
11. 3. 77–25. 3. 77	S1	15	Strombolian eruption of scoriaceous andesite and subordinate juvenile and lithic blocks	2	Peak of discharge from highest level in 1976–1982; vent migrates to floor of crater
25. 3. 77–4. 77		35	Cyclic emission of incandescent juvenile ash and gas; dominantly nonvesicular to moderately vesicular clasts	2	Close of first Strombolian phase; mildly explosive to nonexplosive degassing
Mid to late 5.77		15	Moderate-sized, discrete phreatomagmatic explosions generating pyroclastic fall and surge	2	Renewal of wet explosions clearing tephra that had collapsed and partially blocked the vent
6. 77–7. 77	P2	56	Weak, near-continuous phreatomagmatic eruption involving progressively more juvenile ejecta	2	Widening of conduits by elutriation of lithic ash by increasing volatile flux
late 7. 77.	S2	2–7	Strombolian eruption of scoriaceous andesitic bombs and lapilli and subordinate juvenile and lithic blocks	2	Open-vent eruption from a narrow steep-walled conduit at least 50 m deep
		c.25	Mild pulsating emission of ash, incandescence	2	Mild vesiculation and degassing during waning
25. 8. 77		0.1	Large, discrete phreatomagmatic explosion erupting ballistic blocks; pyroclastic fall and surge	2	Sudden event associated with conduit wall collapse and momentary vent blockage
10. 77		0.1	Moderate-sized, discrete phreatomagmatic explosion generating pyroclastic fall and surge deposits	2	Phreatomagmatic eruption involving more juvenile material than 25. 8. 77
7–8. 11. 77		2	Small discrete phreatomagmatic explosions(s)	3	Similar to above
16. 2. 78–2. 3. 78	P3	15	Near-continuous, mild phreatomagmatic eruptions with progressively more juvenile ejecta	3, 4	Progressive clearance of Gilliver Crater; simultaneous eruption of Christmas Crater
2–16. 3. 78		15	Gibrus-forming event; large, discrete phreatomagmatic eruptions producing ballistic blocks and pyroclastic fall and surge deposits	4	Largest phreatomagmatic eruption and major crater collapse; major modification of geometry of shallow conduits
4. 78–12. 78		280	Relative quiescence		Vent system blocked by Gibrus collapse
24. 12.78–31. 1.79		40	Near-continuous phreatomagmatic eruption involving progressively more nonvesicular juvenile ejecta; rare larger events eject ballistic blocks	5	Progressive establishment of new vent and rapid deepening by removal of ash from conduit

Table 2. (continued)

Date	Phase duration (days)	Description	Source vent (see Fig. 4)	Comments
2. 79–3. 79	60	Near-continuous eruption of angular, non-vesicular juvenile ash	5	Rapid deepening of vent; start of S3 phase
4. 79–5. 79	40	Strombolian eruption of andesitic lapilli and bombs, and subordinate juvenile and lithic blocks	5	Fragmentation surface at least 200 m deep in collimated vent
	S3			
6. 79–10. 80	490	Weakly explosive; near-continuous eruption of juvenile ash, alternating with at least 2 short Strombolian episodes, and rare small phreatomagmatic explosions	6	Alternation of weakly explosive degassing from fragmentation surface at least 200 m deep and rarer, more violent Strombolian explosions
21. 10–2. 11. 80	10	Last open-vent Strombolian eruption, forming thin lapilli fall deposit	6	Last open-vent Strombolian eruption
12. 80–2. 81	90	Near-continuous phreatomagmatic eruptions with moderate-sized, discrete phreatomagmatic explosions on and around 24. 1. 81 (ash fall on mainland)	6	Rapid excavation of partially blocked vent
	Final			
2. 81–9. 81	210	Relative quiescence	6	Infilling of vent by collapse and erosion
9. 81–29. 1. 82	150	Near-continuous, weak phreatomagmatic eruptions; rare larger explosions ejecting blocks and bombs	6	Minor explosive activity accompanying declining magma:water interaction and reduced vigour of degassing

uous ash and gas emission resembling P1. The P2 deposits consisted of lithic-rich ashes of fall and surge origin, totalling some 10^5 m^3 in volume. The S2 phase lasted 20–30 days, with the bulk of the 3×10^5 m^3 deposit accumulating over 2–7 days. The deposits had a similar grain size and axis of dispersal to S1. The third phreatomagmatic phase (P3) was characterised by long intervals of quiescence (50–280 days) alternating with brief, discrete phreatomagmatic explosions. Near-continuous, weakly explosive activity recommenced 2 months prior to the onset of S3 volcanism. The P3 deposits totalled some 10^6 m^3, consisting of laterally continuous, fine-grained fall and surge deposits and discontinuous ballistic block aprons. The S3 phase lasted approximately 600 days, but true open-vent Strombolian eruption was rare. Activity during most of this extended period consisted of rhythmic emission of pulses of gas and blocky, crystal-rich juvenile ash. Rare, volumetrically insignificant phreatomagmatic eruptions occurred. The last Strombolian eruption occurred in October 1980. The final phreatomagmatic phase that followed lasted for 410 days, which included a 7-month interval with little eruptive activity in mid-1981.

Collapse craters

The formation of two maar-like craters during the 1976–1982 eruption sequence is the largest morphological change at White Island since the 1914 crater wall collapse and debris avalanche. The 160-m-wide Christmas Crater formed in early 1977, followed by the 320-m-wide Gibrus Crater in March 1978 (Table 3). These two craters then coalesced to form 1978 Crater Complex with a total volume approaching 10^7 m^3 (Fig. 5). Formation of the new craters was dominated by collapse processes. Christmas Crater formed in the area of the partially coalesced 1933 and 1971 craters. A temperature of 620° C was measured in a strong fumarole on the western wall of 1971 Crater (Giggenbach and Sheppard 1989) on 13 December 1976, 5 days before onset of the eruption. When next observed on 30 December, after 12 days of mild phreatomagmatic eruptions a saucer-shaped hollow had developed in the 1971 Crater, with ash and steam being emitted from a small vent, apparently at the site previously occupied by the fumarole. The hollow developed progressively into a steep-walled crater, 30 m deep on 11 January 1977 and 160 m wide and 100 m deep on 25 January 1977 (i.e. ca. 70 m below sea level). Ash emission during this period occurred from a 10-m-wide vent high on the western wall of the crater. There were few ballistic blocks amongst the predominantly ash-sized ejecta, the vent walls were near-vertical, and the crater rim was surrounded by arcuate slump cracks. Our best estimates of crater and tephra volumes (2×10^6 m^3 and 6×10^5 m^3, respectively) suggested that the crater was considerably larger than the volume of tephra erupted from it. All this evidence suggests that crater growth was dominantly by subsidence and collapse and that substantial void space was present beneath 1971 Crater prior to the onset of eruption. Christmas Crater continued to grow through 1977

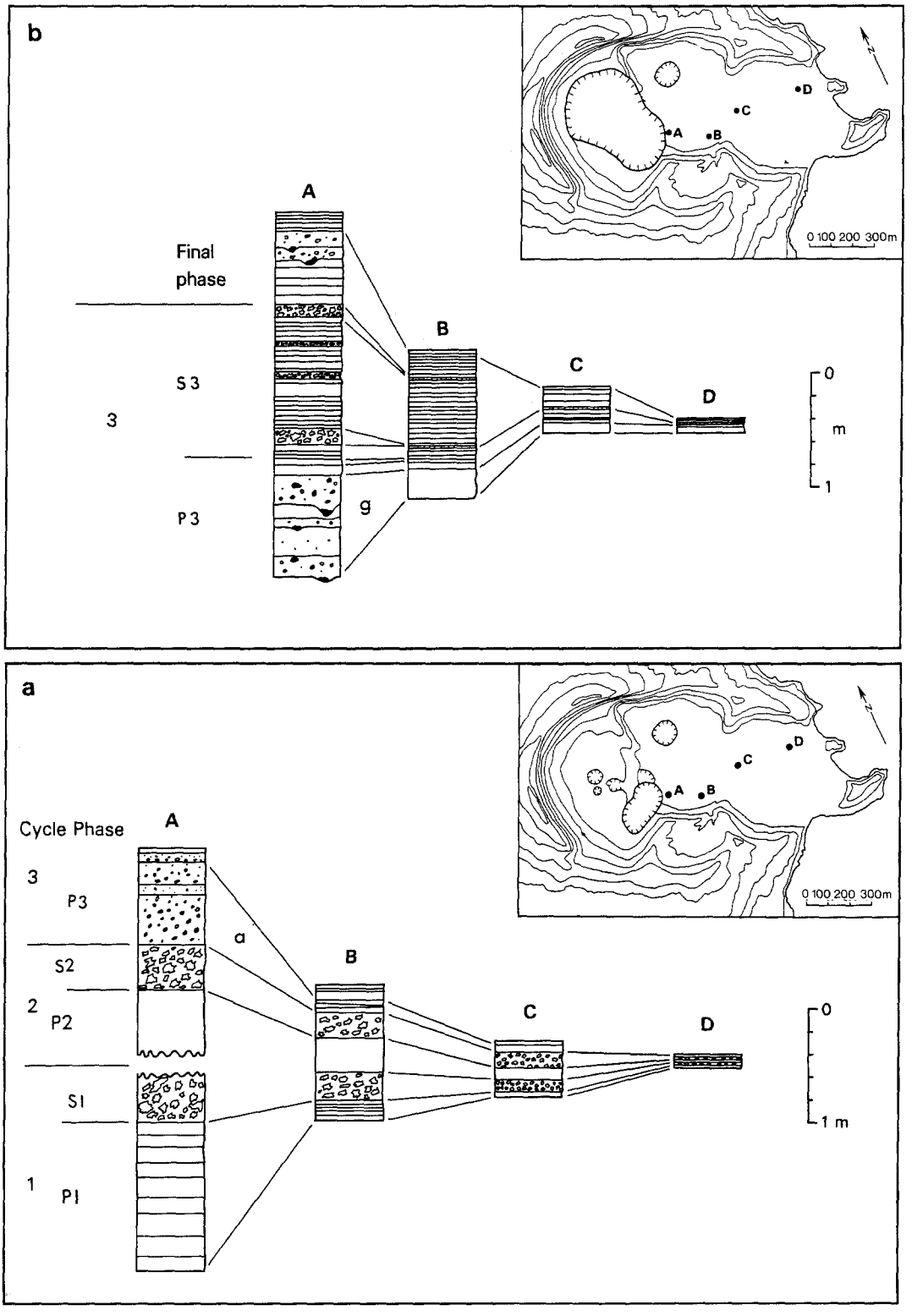

Fig. 3a, b. Summary of stratigraphy for the 1976–1982 eruption sequence at White Island for four sites (*A–D*) on the main crater floor. *S* are Strombolian phases, *P* phreatomagmatic phases. **a** During eruptions from Christmas Crater; **b** following formation of Gibrus Crater. **a** Deposits of the 25 August 1977; **g** deposits from the Gibrus eruption of March 1978 (both phase P3), which are referred to in the text

with further collapse of slump blocks, and the vent migrated to the floor of the collapse crater after the S1 Strombolian phase.

A 50-m-wide pit formed by collapse within Sulphur Crater (Fig. 2) during the 25 August 1977 phreatomagmatic eruptions when a series of concentric steaming cracks opened roughly concentric on Gilliver Crater.

Simultaneous ash emission from Christmas and Gilliver craters in late February 1978 (Fig. 4) was followed by major collapse, forming Gibrus Crater, accompanied by larger phreatomagmatic eruptions. Gibrus Crater incorporated the previous Gilliver, Sulphur and Big John craters, and was 330 m wide and 100 m deep (Fig. 5). A thin ejecta fan formed a sharp ridge separat-

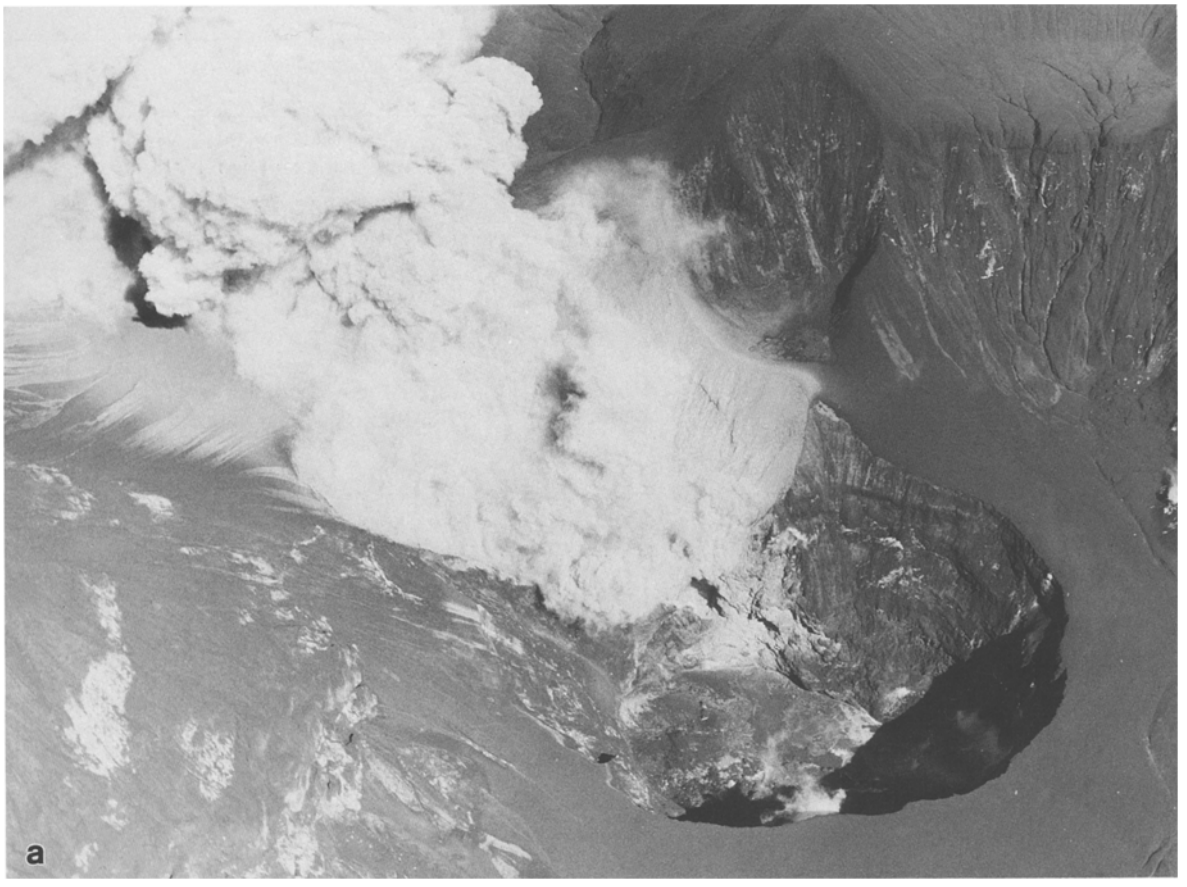

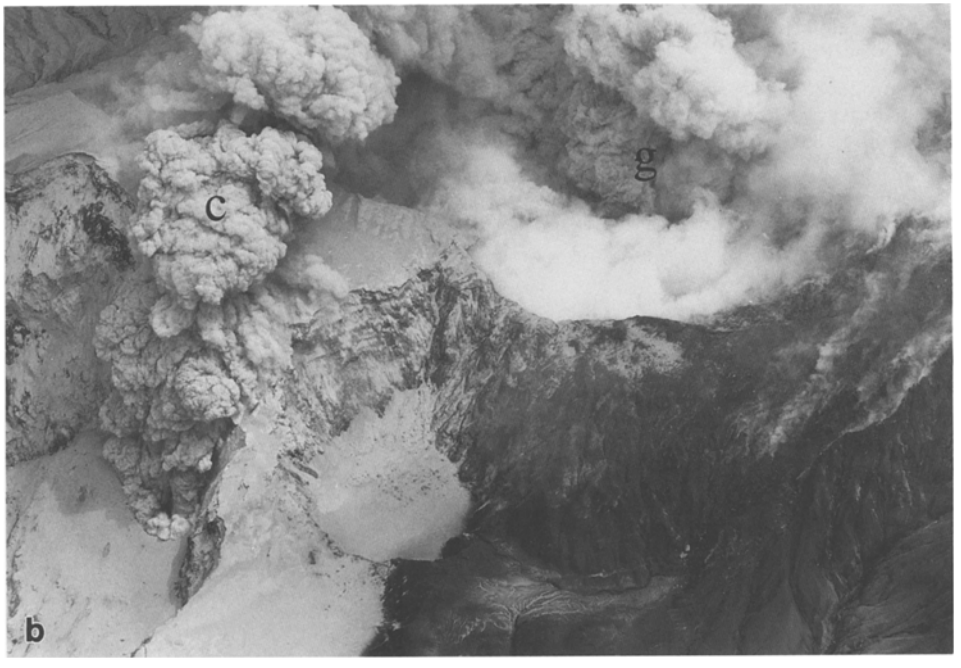

Fig. 4. a Near-continuous emission of gas and ash from a vent on the west wall of Christmas Crater, 12 February 1977. Note the steep-walled and flat-floored form of the collapse crater and the absence of ballistic blocks. Christmas Crater is ca. 160 m wide. Photograph by IA Nairn. **b** Simultaneous eruption from Christmas (*c*) and Gilliver (*g*) craters on 16. 2. 78. Photograph IA Nairn

ing Gibrus and Christmas craters. The volume of Gibrus Crater (7×10^6 m^3) was about 3 times that of Christmas Crater and greatly exceeded the calculated volume for the March 1978 tephra of 4×10^5 m^3. Christmas and Gibrus craters had merged by early August 1978, as a combined result of slumping and minor explosive activity, and the combined feature was renamed 1978 Crater Complex with a total volume approaching 10^7 m^3. The rim of 1978 Crater Complex continued to migrate slowly outwards by slumping of portions of the unstable walls.

Table 3. A chronology of collapse crater development at White Island, 1976–1982

Date	Eruptive phase	Collapse crater development	Dominant processes	Synchronous eruptive activity
8. 12. 76				Eruption commences; small phreato-magmatic eruptions
20. 12. 76		Small saucer-shaped hollow develops as precursor to Christmas Crater		Continuing mild, near-continuous phreatomagmatic eruptions
11. 1. 77	P1	Christmas Crater now wider and 30 m deep	Crater formation	
25. 1. 77		Christmas Crater 160 m wide and 100 m deep		
2. 77–3. 77		Partial infilling of Christmas Crater while active vent widens and migrates down western wall of the collapse crater	Crater infilling	More violent phreatomagmatic eruption, leading to initial part of Strombolian activity
11–25. 3. 77	S1	Vent migrates to floor of Christmas Crater	Crater modification	Climax of first Strombolian phase
25. 8. 77		Christmas Crater unchanged; new steaming cracks develop, concentric on pre-existing Gilliver Crater; partial collapse of floor of pre-existing Sulphur Crater	Crater modification	Major phreatomagmatic eruption
11. 10. 77		Christmas Crater enlarged by collapse/eruption; former active vent blocked by tephra	Crater modification	Minor phreatomagmatic activity
22. 2. 78				Simultaneous phreatomagmatic eruptions from Christmas and Gilliver Craters observed for the first time
28. 2–2. 3. 78		Progressive enlargement of Gilliver and Christmas Craters by wall collapse	Crater formation	Mild-to-moderate phreatomagmatic activity
3. 3.–16. 3. 78		Rapid collapse to produce Gibrus Crater at the the expense of Gilliver Crater and surrounding area	Crater formation	Major phreatomagmatic eruption from a vent within Gilliver Crater
	P3			
4. 78–6. 78		Reworking of tephra and blockage of vent within Christmas Crater	Crater infilling	
29. 6. 78		Two small subsidence pits have formed within Christmas Crater	Relative quiescence	
7. 78		Coalescence of Christmas and Gibrus Crater by collapse and disruption of tephra forming dividing wall; composite structure now renamed 1978 Crater Complex; "Christmas Crater pits" coalesce and deepen	Crater modification	
24. 12. 78		Formation of new vent within former Christmas Crater	Crater modification	Near-continous, mild explosive phreatomagmatic activity
25. 1. 79		New vent is now 200 m wide and >200m deep; eastern wall of 1978 Crater Complex continues to migrate by slumping and collapse	Crater modification	Mild-to-moderate explosive phreatomagmatic activity
26. 5. 80		Three small collapse pits emitting high-temperature gas from 80–200 m east of 1978 Crater Complex		
	S3			
21. 10. 79		Collapse of Christmas Crater portion of 1978 Crater Complex had occurred constricting the active vent	Crater infilling	Modified Strombolian eruption influenced by the deep, steep-walled and narrow form of the vent

Table 3. (continued)

Date	Eruptive phase	Collapse crater development	Dominant processes	Synchronous eruptive activity
2. 12. 80	Final	Active vent had been re-excavated and deepened to +250 m	Crater modification	Several discrete small phreatomagmatic Eruptions with increasingly long intervals of quiescence
1. 81		Progressive infilling of the active vent and development of ponds on the floor of Christmas Crater		

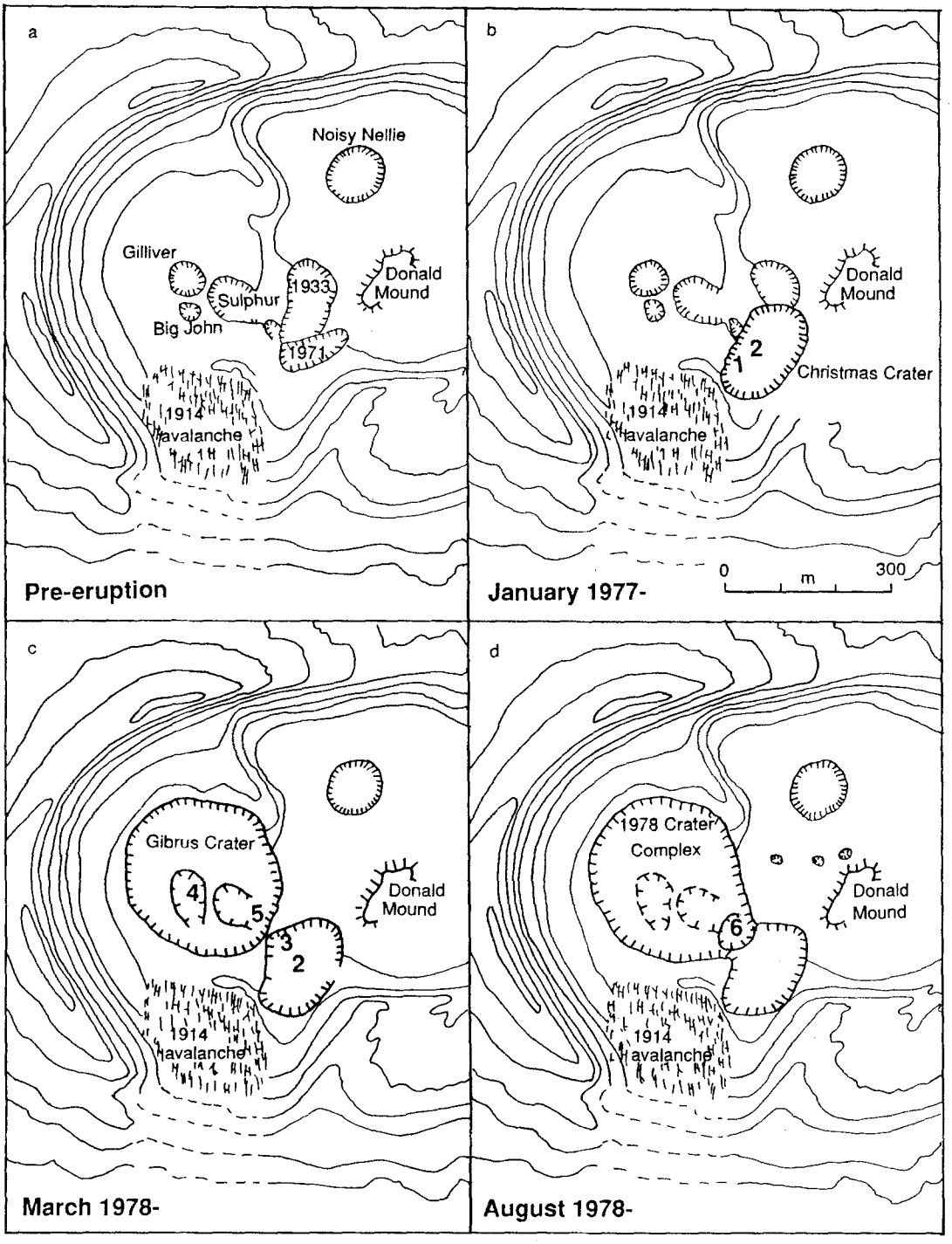

Fig. 5 a–d. Summary of collapse crater and vent geometry during the 1976–1982 eruption of White Island volcano. Vent locations are numbered: *1* December 1976–March 1977; *2* March 1977–November 1977; *3* November 1977–March 1978; *4* February 1978–March 1978; *5* late March 1978; *6* December 1978–January 1982. Note that vents 3 and 4 were briefly in simultaneous eruption

Vent position and dimensions during the 1976–1982 eruptions

A striking feature of the 1976–1982 eruptive sequence was frequent migration in vent positions within the collapse craters (Fig. 5). The vents were generally narrow (< 50 m), steep-sided and deep (50–200 m) pits whose form changed rapidly in response to erosion, wall collapse and infilling. Initial vent position was high on the western wall of Christmas Crater (Fig. 4a, Vent 1 on Fig. 5). This vent migrated 60 m eastward during the first Strombolian phase in March 1977 to the floor of the collapse crater (vent 2, Fig. 5). Collapse blocked this vent with debris in November 1977, and emission resumed in February 1978 from vent 3, formerly a fumarole on the northwestern wall of the crater close to or at the former site of Rudolf Crater (Fig. 5). By late February 1978 ash was being emitted simultaneously from this vent and vent 4 in Gilliver Crater, 200 m to the northwest. After collapse of Gibrus Crater, eruptions took place from a pit in Christmas Crater, again close to the Rudolf site. Collapse and subsidence blocked this vent in April–May 1978 and two new pit-vents formed on the northern and western floor of Christmas Crater. These pits had coalesced and deepened by August 1978 (forming vent 5), and were replaced in December 1978 by vent 6, at the Rudolf site again, which was now part of the extended 1978 Crater Complex. This vent developed rapidly, forming a subcrater 200 m wide and more than 200 m deep by January 1979. Collapse prior to October 1980 reduced this vent to a 10- to 20-m-wide pit slightly southeast of its former position. Vent 6 was enlarged to its previous width and a depth of at least 250 m by December 1980, and then was progressively infilled to shallower levels throughout 1981 and 1982.

In summary, vent position migrated six times during the eruption sequence, in response to eruptions, formation of collapse craters, and superficial slumping, but was repeatedly re-established on a line joining the pre-existing Gilliver and 1933/1971 craters.

Phreatomagmatic volcanism

We distinguished two styles of phreatomagmatic eruption in 1976–1982: weak, near-continuous gas and ash emission and larger, intense, discrete phreatomagmatic explosions. Near-continuous emission occurred for periods of weeks or months, with dilute pulses of ash and gas emitted at frequencies as high as 1/s. Emission velocities were generally less than 50 m/s, with pulses already expanded and weakly convecting when first visible in the vent (Fig. 4). Column heights were low, generally 0.3–1.0 km. Only minor modifications to the geometry of the vents and collapse craters occurred during these periods.

The large discrete explosions ejected ballistic lithic blocks and abundant finer clasts, accompanying eruption columns several kilometres high. They occurred somewhat randomly, following directly after either periods of quiescence, or mild near-continuous phreatomagmatic intervals, or (on one occasion) Strombolian eruption. However, they were invariably followed by intervals of quiescence lasting up to 4 months. Most major topographical modifications of the collapse craters accompanied larger phreatomagmatic events.

Not all phreatomagmatic phases at White Island were equally well recorded because of weather conditions, the distance from the mainland, and technical difficulties with monitoring equipment. Below we describe two well-observed eruption intervals, which typify the styles of phreatomagmatic volcanism.

Large phreatomagmatic eruption: 25 August 1977 (P3)

A large discrete phreatomagmatic event on 25 August 1977, which represented the abrupt start of the P3 phase, was observed by a pilot on a tourist flight over White Island. At this time the active vent was a narrow circular pit on the floor of Christmas Crater (vent 2 on Fig. 5). The pilot had noticed incandescence in the vent 8 min before the eruption; this formed part of the final degassing stage of the S2 Strombolian phase. Two explosions were witnessed 15 min apart. Each ejected a range of material including fine ash and blocks, a few of which were incandescent. Fine ash from the 5-km-high convective column was dispersed north-northwestwards by a 30 km/h wind. A total of 1×10^5 m^3 of ejecta containing < 2% juvenile material was erupted. The remainder of the deposit was derived from the hydrothermally altered tephra and volcaniclastic sediments that infill the main crater. Ballistic blocks fell over a wide area extending at least 800 m from the vent. The remainder of the ejecta formed two pairs of pyroclastic surge and fall deposits (Fig. 6). The fall deposits were very poorly sorted but coarser-grained than the very fine-grained and poorly sorted surges (Fig. 7a). The fall units thinned and fined dramatically (Fig. 7b) down the main crater (i.e. upwind). Surge deposits were more extensive, forming a thin sheet across the main crater floor, ending abruptly 900 m from the crater. Ash coated even the exposed undersurfaces of blocks, indicating deposition in a wet sticky state, and wooden and cardboard objects were unaffected, implying low emplacement temperatures. Low transverse dunes of several centimeters amplitude were present on the upper surface of the surge deposits within 250 m of the vent, and the deposit was noticeably crossbedded beyond this. Billowing, dilute clouds of ash and gas were observed rising from the flowing surges and these deposited a millimeter-thick layer of fine ash to heights of 200 m on the walls of the main crater. Collapse of crater-filling sediments infilling the eroded remnants of Sulphur Crater (Fig. 5) and development of new steaming cracks concentric on Gilliver Crater accompanied the eruption. Part of the Sulphur Crater fill flowed across the surface as a mudflow, but most of it collapsed into the conduit system beneath the crater(s). The eruption was followed by 2 months of quiescence.

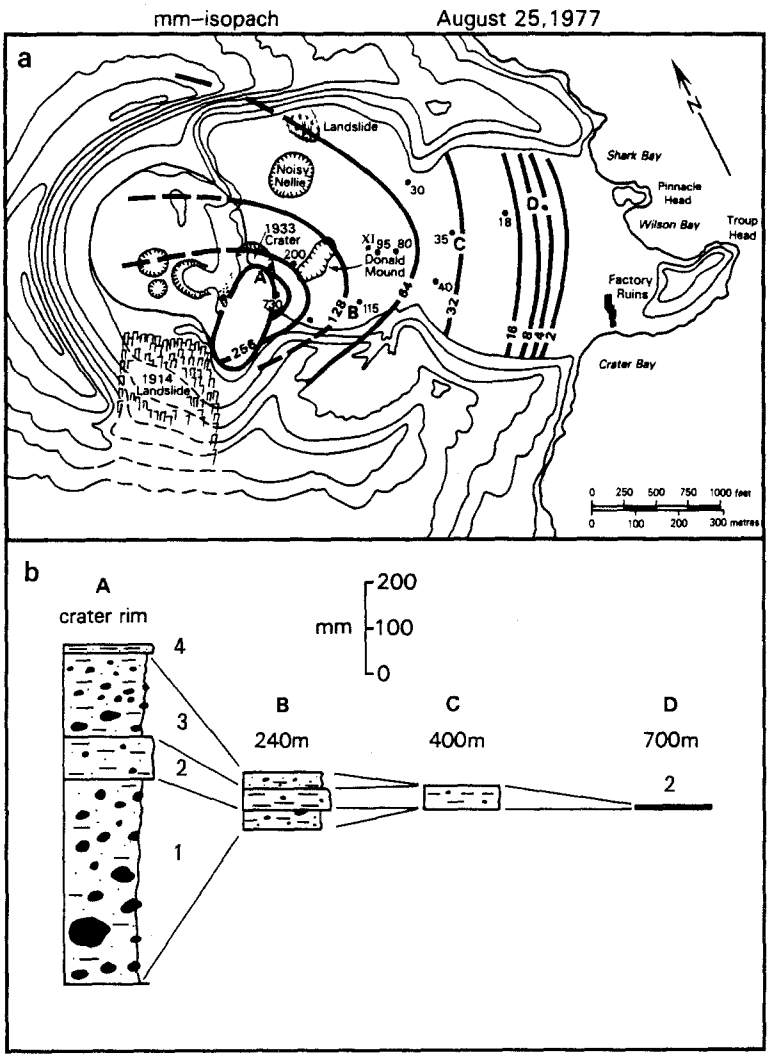

Fig. 6. a Isopach map for the 25 August 1977 phreatomagmatic eruptions. *Note* the change of radius of curvature at the 64 mm isopach beyond which only surge deposits are present. Thicknesses an in millimeters. **b** Stratigraphic sections through the deposits at sites *A–D* in **a**. 1, 3 = fall deposits, 2, 4 surge deposits

Weak, near-continuous eruption December 1978–January 1979 (P3)

This time interval typified the style of near-continuous phreatomagmatic gas and ash emission. A new vent became established on the floor of 1978 Crater Complex during these eruptions and rapidly deepened and widened, reaching a depth of 50 m by 25 January 1979 (vent 6 on Fig. 5). Emission was near-continuous at this time, generating a dilute, weakly convecting column rising to 400–600 m. There was a strong wind influence on deposition, with individual beds overthickened on the upwind side of obstacles, mimicking the form of surge deposits. A mixture of both dry and wet ash fall occurred, with wet ash falling both as damp clusters or aggregates, and in acidic ash-charged water droplets. Rarely, more violent pulses emitted lithic lapilli and occasionally ballistic blocks. Even small lapilli penetrated to several centimeter depths in the loose, unconsolidated ash. The deposits of this period consisted of expanded, laminated, very poorly sorted fine ash, which increased markedly in its juvenile content between December and January. The deposits were both fine-grained and very poorly sorted (Fig. 8).

Phreatomagmatic deposits

The large discrete phreatomagmatic eruptions produced three types of deposits: ballistic block aprons, cohesive surge deposits and downwind lobes of fall deposits (Houghton et al. 1989). The three products typically had distinctive distributions (Fig. 9). Ballistic block aprons were generally near-circular about vent. However, on rare occasions, when eruptions took place form deep within a steeply inclined vent the blocks were collimated into a restricted fan-shaped configuration. Most blocks were found within impact craters, buried in earlier unconsolidated tephra. Occasionally, when eruption followed quiescence and extensive erosion and compaction, blocks bounced off the indurated substrate and were found up to 30 m from the associated impact craters.

Fall deposits from the convective portion of eruption columns were controlled by the variable wind conditions. The accompanying surges were channelled south-southeastward along the main crater floor and deposited ash at a range of temperature. Most were wet-depositing cohesive material that typically coated the craterward faces of obstacles and was absent from

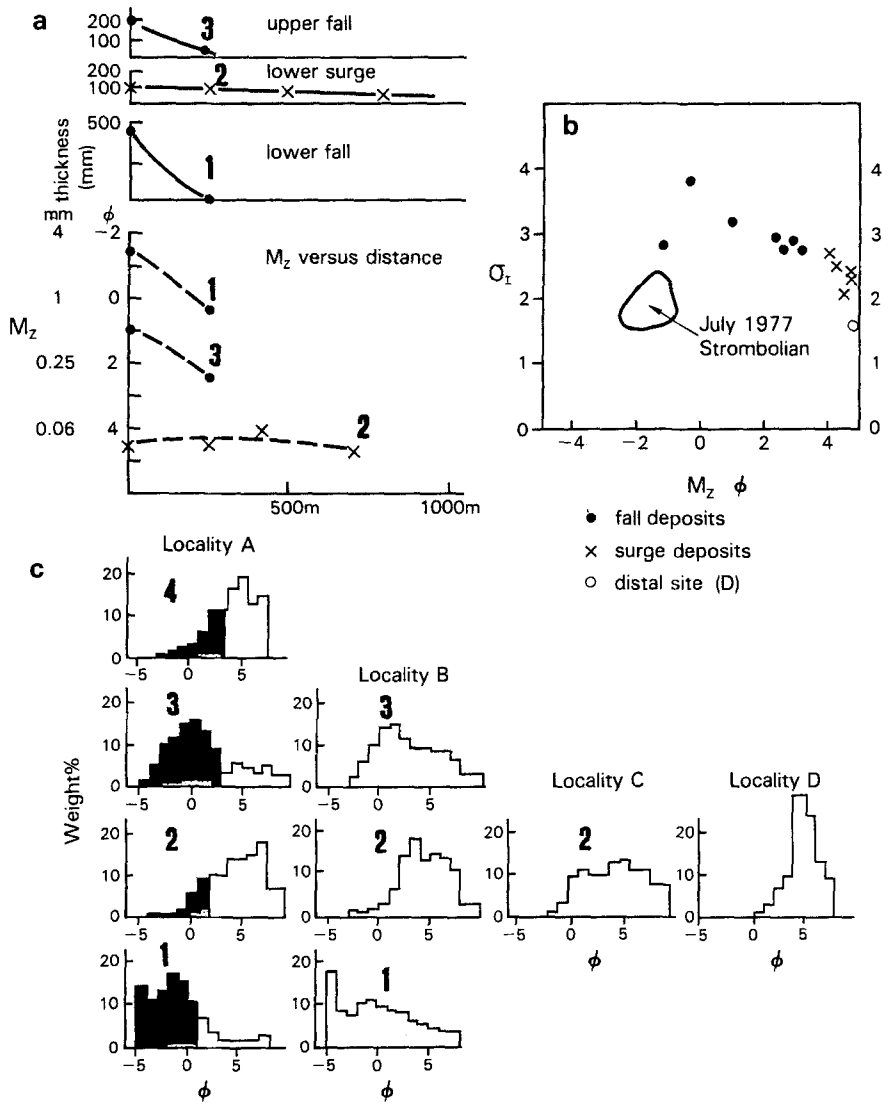

Fig. 7. a Plot of thickness and graphic grain size means against distance from crater rim for the 25 August 1977 deposits. *1, 3* Fall deposits; *2* surge deposit. **b** Plot of graphic mean versus inclusive graphic standard deviation for the 25 August 1977 phreatomagmatic deposits. The field of S2 Strombolian deposits is outlined for comparison. **c** Grain-size histograms and component analysis for the 25 August 1977 deposits. *Black* represents wall rock lithic material; *stipple* juvenile vitric clasts. *Open areas* not separated into components

shadow zones behind them (Fig. 10a). A few were dry (> 100° C), and deposits remained hot and fluidised for some days after deposition. Streamlines of u-shaped dunes were formed behind obstacles in the hot dry-surge deposits (Fig. 10b).

Both fall and surge deposits are typically fine-grained and very poorly sorted (Figs. 11, 12). In individual eruptions the grain-size characteristics of fall and surge deposits are often very similar, and fall units may show the poorer sorting (e.g. Fig.12b); however, fall units invariably thin out and fine much more rapidly with distance from the source (Fig. 12b-d).

The small, near-continuous phreatomagmatic eruptions produced complex deposits unsuited to conventional stratigraphical analysis. A variety of fall mechanisms operated, with often both 'dry' and 'wet' accumulation of ash (Fig. 13). Some eruptions produced dry-ash fall close to the vent and simultaneous distal rainout of wet aggregates of ash. At other times dry-ash fall from the column was followed by wet fall at the same site. The final product of an interval of numerous pulses was a poorly sorted laminated bed with small lapilli set in a fine-ash matrix (Fig. 13).

The principal component of the phreatomagmatic deposits are lithic clasts derived from the conduit walls (Figs. 7, 12). This lithic component was dominated by hydrothermally altered tephra dominated by kaolinite-alunite-anhydrite-silica recycled from earlier phases of this and previous eruptions. The pre-existing fine grain size and unconsolidated nature of the country rock imparted a strong bias to the grain size of the 1976-1982 phreatomagmatic deposits. The minor component of juvenile clasts increased systematically throughout each of the phreatomagmatic phases. The rapid and intense acidic hydrothermal alteration in the vent area meant there was seldom any problem in distinguishing fresh juvenile clasts from recycled material. Acid attack on juvenile clasts continued after samples had been enclosed in plastic bags, necessitating rapid collection and component analysis after each eruption. Juvenile clasts in each cycle were initially angular and nonvesicular, but both nonvesicular and vesicular shards were present in the latter stages of each phreatomagmatic phase.

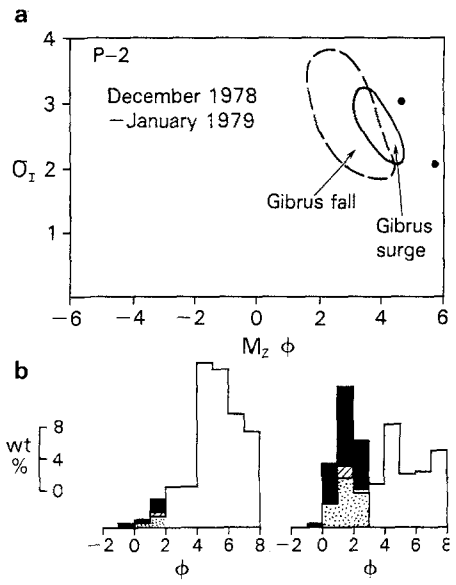

Fig. 8a, b. Characteristics of P3 phreatomagmatic deposits, December 1978–January 1979. **a** Plot of graphic mean versus inclusive graphic standard deviation for two samples. Fields of deposits for the large, discrete phreatomagmatic eruptions associated with the formation of Gibrus Crater during phase P2 and included for comparison. **b** Grain-size histograms and component analyses. *Stipple* represents juvenile glass; *diagonal hatching* juvenile crystals; *black* accessory lithics

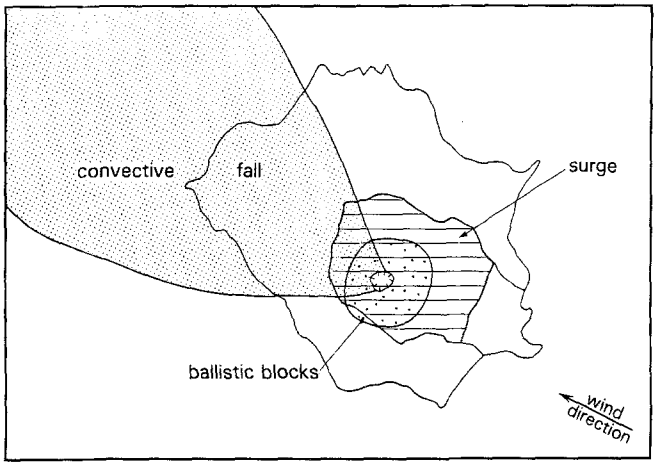

Fig. 9. Distribution of pyroclastic surge and fall deposits and ballistic blocks from a typical large discrete phreatomagmatic eruption at White Island

Strombolian volcanism

The magmatic phases of the 1976–1982 eruptions began with intervals of weakly explosive degassing and eruption of blocky juvenile ash derived from the margins of the magma body. Open-vent Strombolian eruption then followed, but its duration and the resulting deposits in each cycle depended on the vent geometry and the depth to the fragmentation surface at the top of the magma. These depths could not be accurately measured, but the fragmentation surface was at or close to the level of the main crater floor during S1, at least 50 m deeper in S2, and more than 150 m deeper during S3 (Fig. 14). During S3 the vent was within a deep subcrater nested within 1978 Crater Complex. When open-vent Strombolian eruption did occur, large clasts were collimated on near-vertical trajectories and most fell back in the vent.

The close of Strombolian phases was marked by a return to weakly explosive degassing and emission of incandescent pulses of gas and blocky juvenile ash. Two well-observed and representative examples of the range of Strombolian behaviour are described below.

Open-vent Strombolian eruption: late July 1977 (S2)

The S1 phase best typified open-vent Strombolian activity at White Island, but its products were rapidly buried and were studied in less detail than the S2 deposit, which we have chosen as a representative example of this eruptive style. The S2 eruption lasted at the most only 7 days, erupting 3×10^5 m^3 of tephra. During its climax on 29–30 July 1978, fine ash was deposited on the mainland 65 km distant. The eruption took place from a vent on the floor of Christmas Crater and was unaccompanied by any change to the vent area. The S2 deposit was a single, massive, well-sorted bomb and lapilli bed, 370 mm tick on the rim of Christmas Crater, with an eastward axis of dispersal (Fig. 15a). It was dominated by highly vesicular basic andesite scoria, but with lithic blocks and lapilli concentrated at the top of the deposit. The lithic clasts included massive nonvesicular juvenile basic andesite, and both baked and acid-altered fragments of wall rock. The largest blocks and boms were 1 m in diameter.

The main Strombolian phase was succeeded by pulsating, weakly explosive degassing and eruption of blocky nonvesicular juvenile ash. This material rapidly infiltrated pore spaces in the clast-supported bomb and lapilli bed. The degassing lasted 3 weeks before the abrupt commencement of the P3 phreatomagmatic phase.

The S2 deposits were noticeably coarser and better sorted than preceding phreatomagmatic deposits (Fig. 15c). Channel samples for grain-size analysis were bimodal, with the principal peak produced by scoria and a coarser subordinate peak due to the late stage lithic lapilli (Fig. 15b).

Modified Strombolian eruption May–August 1979 (S3)

This interval was chosen as typical of the modified Strombolian eruptive style, which prevailed during S3 volcanism. The vent at this time was a subcrater on the floor of 1978 Crater Complex, which had reached a depth >200 m. Eruption consisted of pulses of gas and ash emitted at intervals of 5 to 30 s. The largest pulses were accompanied by audible detonations and ejected incandescent bombs and blocks up to 1 m in diameter. These rose to heights of up to 100 m above the rim of

Fig. 10. a Wet pyroclastic surge deposits on the vent-facing side (*left*) of a projecting block. Note desiccation cracks in the originally wet ash. **b** Streamlined deposition of ash behind a projecting block. Direction of flow is towards the viewer. Dry pyroclastic surge deposit, 25 May 1977. Photograph by IA Nairn

1978 Crater Complex, but followed near-vertical trajectories, falling back into the crater. Most pulses emitted only fine ash, consisting of juvenile crystals and subordinate amounts of nonvesicular and pumiceous glass, in weakly convective columns rising 300–600 m above the floor of the main crater. The deposits consisted of bedded fine ash with 3-cm-thick coarse ash – fine lapilli bands (Fig. 16). The beds were locally dispersed, with significant accumulation only within 200 m of the crater rim, but on the rim observed accumulation rates locally reached 3–5 mm/min. The ash deposits were fine-grained but significantly better sorted than the products of phreatomagmatic phases of the 1976–1982 eruptions (Fig. 17).

Strombolian deposits

The Strombolian lapilli and bomb beds produced during open-vent eruption were coarse-grained and relatively well sorted (Fig. 11). They were dominated by juvenile scoria consisting of fusiform, cow dung and rib-

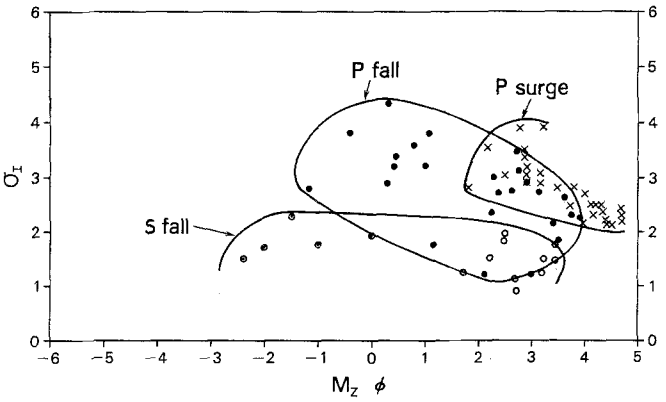

Fig. 11. Summary of grain-size data from 1976–82 tephras. *Open circle with dots* S1 and S2 Strombolian deposits. *Open circles* magmatic deposits of S3 Strombolian phase. *Closed circles and crosses* are fall and surge deposits, respectively, of the phreatomagmatic phases (*P*), after Houghton et al. (1989)

bon bombs and more compact bread-crusted but vesicular bombs (Fig. 18). Subordinate dense juvenile blocks contained zones of fused glass inferred to be produced by gas-fluxing. The ashes that accumulated during the start and end of the S1 and S2 phase and during most of S3 were well sorted (Fig. 11). The ash was transported and deposited in a dry disaggregated state with very efficient fractionation into proximal crystal-enriched and distal vitric-enriched facies. A range of vesicularity among the vitric clasts indicated that explosions involved both relatively degassed and/or quenched margins to the magma body, as well as its actively degassing interior.

Interpretation and model

Subsurface structure and hydrology

The three prehistoric subcraters that make up the main crater floor at White Island are partially infilled by reworked pyroclastic and epiclastic material, including the 1914 debris avalanche (Figs. 19, 20). The subcraters are inferred to have formed by a combination of explosive eruption and crater collapse similar to those observed in 1976–1982. The subcrater fill is water-saturated but impermeable material cut by volcanic conduits, which are regions of high, vertical permeability utilized by the acidic hydrothermal system beneath White Island (Giggenbach 1987). Trace-metal distribution in marine sediments around the island indicates that hydrothermal activity has been sustained for at least 10000 years (Giggenbach and Glasby 1977), presumably driven by the deep magmatic body beneath the volcano. The hydrothermal system has formed by reaction of exsolved magmatic volatiles and condensates with meteoric groundwater (Giggenbach 1987).

Although White Island is surrounded by sea, there is no isotopic evidence for sea water interaction with the magmatic system (Giggenbach 1987), probably because of chemical sealing of the margins of the hydrothermal system by precipitation of anhydrite and calcite from heated sea water (Tomasson and Kristmannsdottir 1972; Fournier 1987). The sealed zone that excludes seawater also confines fumarolic condensates and meteoric groundwater obtained from the catchment areas of 0.4 km^2, draining directly into the western subcrater and 3.4 km^2 for the entire island (Fig. 19). The rainfall is probably equivalent to 4000 tonnes/day (Houghton and Nairn 1989c). The brine-saturated but relatively impermeable deposits infilling the subcraters are cut by the volcanic conduits enclosed by successive envelopes of gas and vapour, and two-phase mixtures of gas and vapour plus brine (Figs. 19, 20).

Nature of the White Island conduit system

Prior to 1976, the unconsolidated fill of the western and central subcraters was perforated by a network of narrow conduits leading to the sites of earlier eruptions (Fig. 5). These conduits had been infilled at shallow levels by wall-collapse and fall-back of late-stage ejecta, but must have remained open at depth, as the conduits were the foci for activity in 1976–1982. There is also previous evidence for interconnections between some conduits, in the form of simultaneous ash emission from two different sets of vents in 1959 and 1968 (Martin 1959; Healy 1968). A similar observation was made in February 1978 when Christmas and Gilliver craters were in simultaneous eruption (Fig. 4b). The pre-existing conduits acted as channelways for steam and magmatic gases in 1976–1982 and controlled the location of vents during the eruptive sequence. Four pre-existing conduit systems played significant roles during the eruption, at the sites of 1933/1971 craters, Donald Mound, Sulphur Crater and Gilliver Crater (Figs. 2, 5).

Minor steam eruptions in 1971 Crater in October 1975 suggest reopening of the pre-existing conduit to this area well before the start of the 1976–1982 eruptions. Intense deformation was localised in this region in 1973–1976, and formation of the new high temperature fumarole at the site of vent 1 (Fig. 5) suggests that magmatic volatiles, and ultimately magma, were preferentially channeled into this 1971 Crater conduit.

Donald Mound has been a site of continuously active hot fumaroles throughout historical time, but without significant eruptive activity. Deformation prior to and during 1976–1982 was often localised at Donald Mound (Clark and Otway 1989), and this conduit acted as a channelway for phreatic steam and volatiles escaping from the andesitic magma, without becoming an explosive vent. Collapse of an old conduit system beneath Sulphur Crater into the adjacent conduit of Christmas Crater on 25 August 1977 triggered the largest individual phreatomagmatic eruption of the eruptive sequence. A pre-existing conduit system beneath Gilliver Crater was cleared in February 1987 and the formation of Gibrus Crater followed.

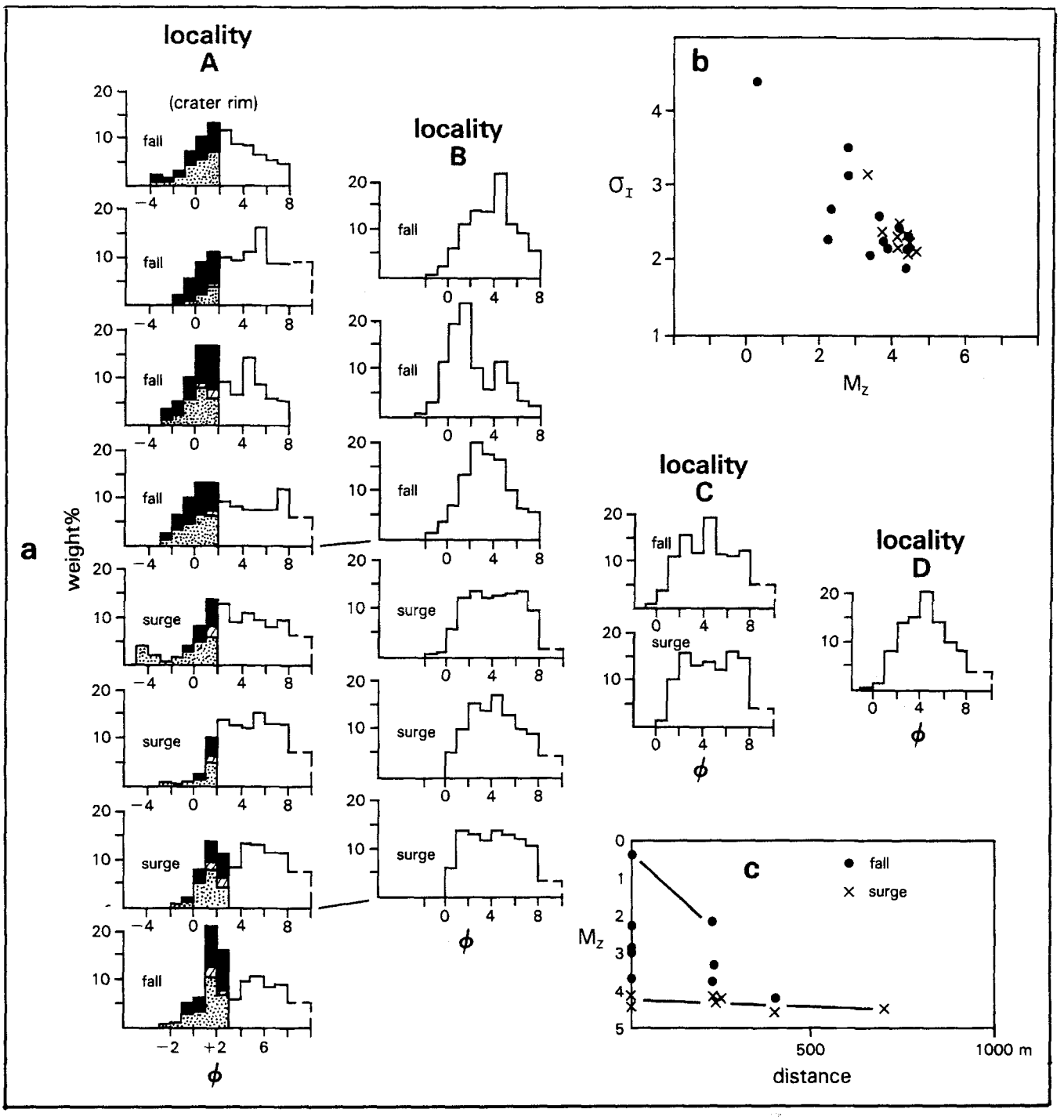

Fig. 12a–c. Grain-size characteristics of phreatomagmatic deposits associated with formation of Gibrus Crater during phase P3. **a** Grain-size and component analyses of samples from sites *A–D* (see Fig. 3). *Stipple* represents juvenile glass; *diagonal hatching* juvenile crystals; *black* accessory lithics. **b** Plot of inclusive graphic standard deviation against graphic mean for fall (*dots*) and surge (*crosses*) deposits. **c** Variation in graphic mean of tephra samples with distance from vent

Rate and form of magma emplacement

Some constraints on the timing of shallow magma emplacement can be obtained from the monitoring data. The magnetic data (Christoffel 1989) suggest widespread heating at depths of 600–800 m from mid-1973 onwards, with high temperatures maintained until well after the close of the eruption sequence in 1982. The deformation data are consistent with magma emplacement to depths of 1–2 km by 1973, followed by more localised rapid intrusion to depths of less than 500 m from 1973–1976 (Clark and Otway 1989). This is consistent with the magma being confined above this level to a more restricted feeder system in the general area of 1971 Crater and Donald Mound (Fig. 20). Above 500 m, this feeder appears to have branched into the

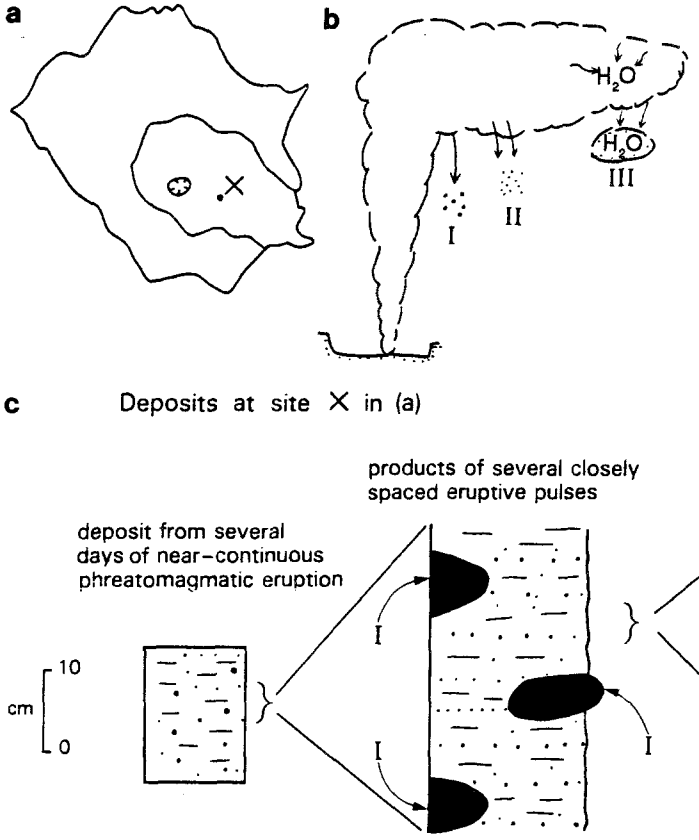

Fig. 13a–c. Schematic section showing products of near-continuous mild phreatomagmatic eruptions. At a given proximal site (× in **a**) any given eruptive pulse may deposit lapilli (*I*), then dry (*II*), and then wet ash (*III*) (**b**). The lapilli settle through the soft ash to depths of several centimeters below the syn-eruptive ash. The result is a complex, massive, and poorly sorted unit that is a composite product of numerous eruptive pulses (**c**)

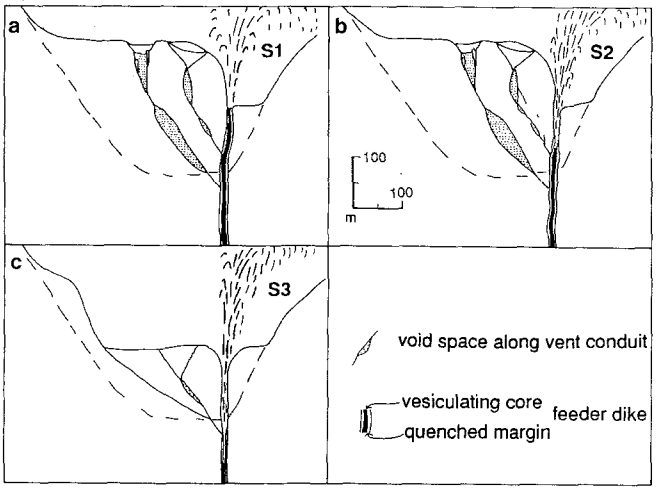

Fig. 14a–c. Schematic sketch showing vent geometry and level of the fragmentation surface during successive Strombolian phases

two narrow conduits beneath these two features. Magmatic volatiles, and ultimately magma, were preferentially channelled into these conduits. Although a significant proportion of the magmatic volatiles escaped through the Donald Mound vents, particularly when alternative routes were blocked by crater collapse (e.g. March 1978), magma followed the more direct route beneath the pre-1976 craters, originally 1971 and 1933 craters, in the western subcrater. The peak of magma advance was in March 1977 at the time of the S1 Strombolian eruption, and both direct observations and the deformation data suggest that the magma then retreated between mid-1977 and 1982 (Houghton and Nairn 1989c; Clark and Otway 1989). As a first approximation, it appears that magma advanced by at least 500 m in the 4 years between 1973 and 1977 and then retreated at least 250 m between 1977 and 1980.

Controls on Strombolian volcanism

Strombolian volcanism at White Island was influenced by the stability of the unconsolidated walls of the vent(s) and conduit(s) and by a complex relationship between the rise rate of magma, its discharge rate and the rise rate of bubbles through the magma. There is clear evidence that magma and magmatic volatiles were decoupled at shallow depths at White Island, in the manner proposed by Vergniolle and Jaupart (1986) and Jaupart and Vergniolle (1988). The long-term flux of SO_2 at White Island following the 1976–1982 eruption (Rose et al. 1986) is equivalent to degassing of ca. 1 m^3/s of andesitic magma containing 0.1 wt% SO_2. Magma discharge rates during the 1976–1982 eruptions probably only reached 1 m^3/s for short intervals at the peak of the S1 and S2 Strombolian phases and averaged 10^{-2} m^3/s over the duration of the eruption. This means effectively far more magma was degassed during and after the 1976–1982 eruption sequence than was ever discharged from the subaerial vents. This can be satisfactorily explained in terms of the relative rise rates of (1) magma and (2) bubbles within the magma. The average rise rate of magma between 1973 and 1977 was

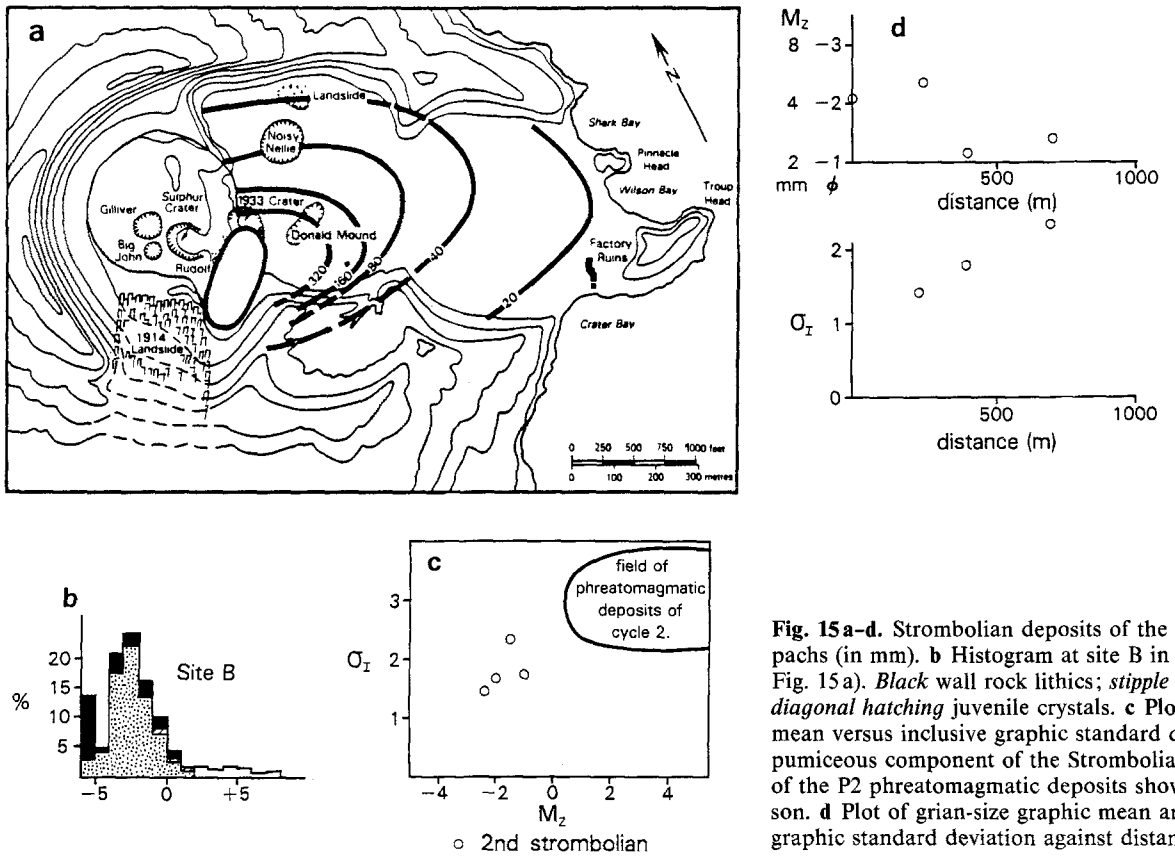

Fig. 15a–d. Strombolian deposits of the S2 phase. **a** Isopachs (in mm). **b** Histogram at site B in Fig. 3 (see *dot* in Fig. 15a). *Black* wall rock lithics; *stipple* juvenile scoria; *diagonal hatching* juvenile crystals. **c** Plot of graphic mean versus inclusive graphic standard deviation for the pumiceous component of the Strombolian deposits. Field of the P2 phreatomagmatic deposits shown for comparison. **d** Plot of grian-size graphic mean and inclusive graphic standard deviation against distance from vent

ca. 3×10^{-6} m/s (Houghton and Nairn 1989b). Rise rates for 1-cm bubbles can be modelled (Murase and McBirney 1973), assuming magma viscosity of 10^4 to 10^5 poise, as 10^{-3}–10^{-4} m/s. This velocity contrast led to effective decoupling of magma and exsolved volatiles and gas streaming during 1976–1982 and during the lead-up to the eruption.

Deformation data suggest the magma reached its highest level during the first Strombolian phase in late March 1977 (Clark and Otway 1989). Observations of incandescence suggest that the magma was relatively deep in the vent in early March and was relatively close to the surface by 4 April 1977, suggesting the rise of new magma exceeded the discharge rate during the climax of the first Strombolian phase. However, by the close of S1, the magma supply had decreased, magma in the conduits had become partially degassed, and degassing was continuing passively without eruption of significant volumes of magma. The second and third Strombolian phases took place during widespread deflation of the island, presumably in response to magma withdrawal at depth. The question of what triggered the S2 and S3 phases is obscured by a lack of deformation data from the vent area, where survey pegs were destroyed in December 1976 and not replaced until December 1981. Without information from this region it is impossible to exclude short-lived advance of magma in the shallow conduit system to initiate S2 and S3. However, this seems unlikely at a time of more widespread deflation, and a more likely alternative is the arrival of fresh pulses of volatiles at the fragmentation surface due to a complex pattern of magmatic degassing at greater depths.

The vigorous, open-vent period within S2 appears to have ended for similar reasons to S1, namely declining magma supply and/or progressive depletion of volatiles in the magma within the vent. The weakly explosive degassing that followed was abruptly terminated by wall collapse.

S3 began after phreatomagmatic explosions had re-excavated a subcrater that exposed the magma surface at a considerable depth beneath the crater floor (Fig. 14c). The deposits were dominated by the great depth to the fragmentation surface. Mild Strombolian explosions disrupted both actively degassing and stagnant degassed magma and ejected both new and recycled bombs, blocks and lapilli. Most of this material fell back into the vent, and only ash-sized clasts rose higher in the eruption columns to form fall deposits on the island. On only six brief occasions did more vigorous eruptions deposit scoria lapilli on the main crater floor. The difference in dispersal of these lapilli beds and the ash fall deposits reflects the relative roles of vent geometry and column height. The lapilli beds have a distribution governed by a steep inclination of the vent that collimated discharge; the ash-sized component rose higher in the dilute convective columns and was dispersed northwards by the wind.

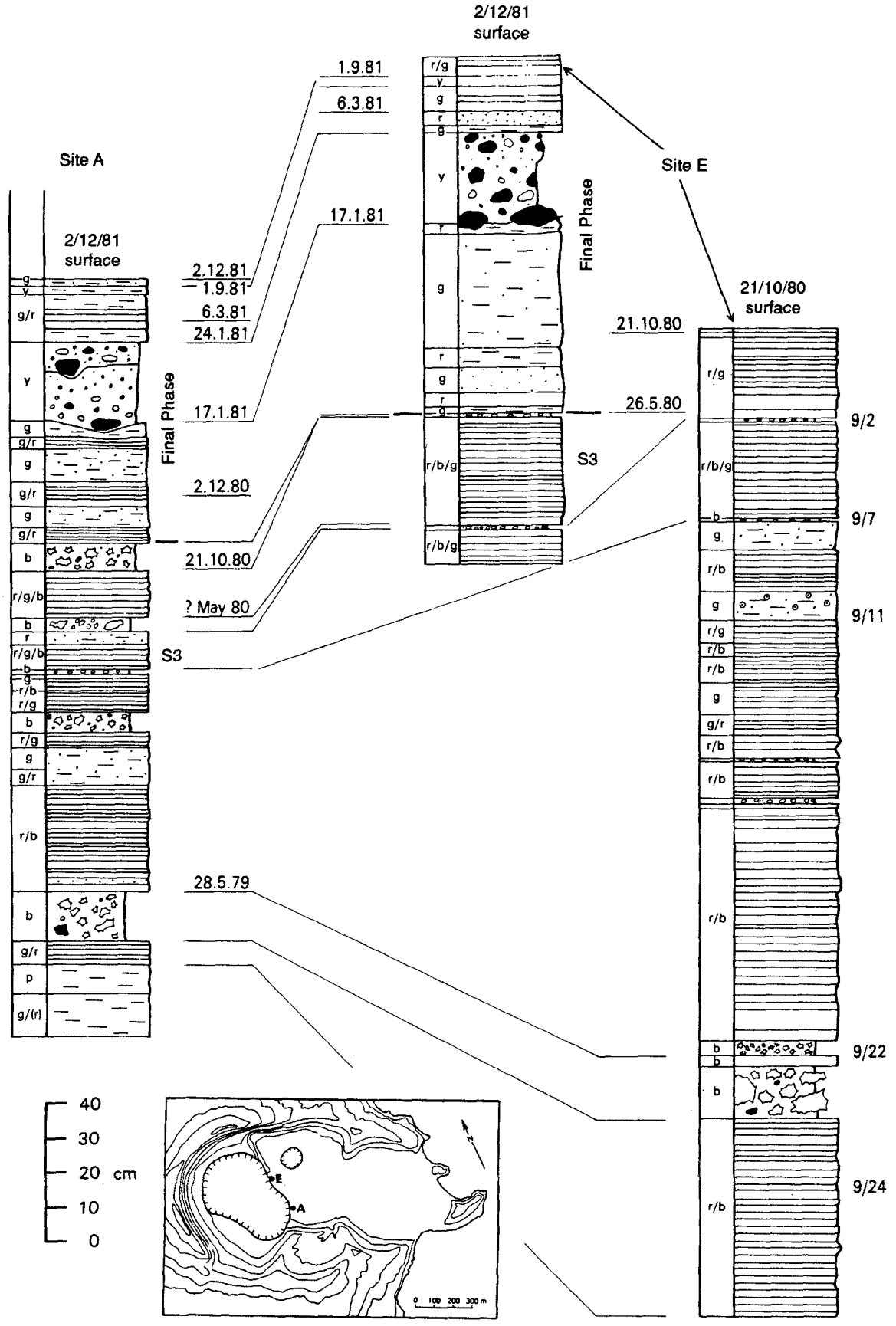

Fig. 16. Stratigraphy of deposits of the S3 and final phases at two sites on the rim of 1978 Crater Complex. The 'open vent' Strombolian lapilli beds are dispersed aong axes close to *site A*, whereas the crystal-rich ash units are thickest at *site E* and thin dramatically towards *A*. The colour of units is given by letter symbols at the *left of the columns*. *b* Brown; *g* grey; *p* purple; *r* red; *y* yellow

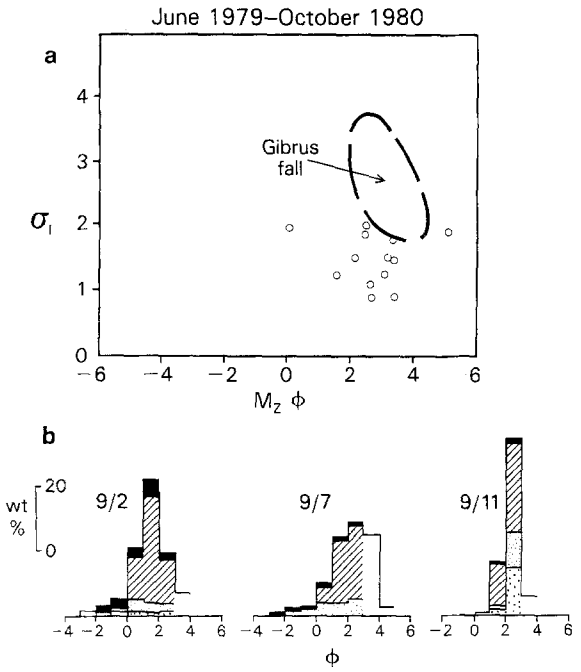

Fig. 17. a Plot of graphic mean versus inclusive graphic standard deviation for May–August 1978 S3 deposits. **b** Grain-size histograms and component analyses for representative samples. Note the extreme crystal enrichment. Symbols as for Fig. 15

Formation of collapse craters

Both major collapse craters formed dominantly by subsidence. Ejecta: crater volume ratios suggest that substantial void space existed within the 1933–1971 conduit system prior to the 1976–1982 eruptions (Fig. 21a). These shallow void spaces probably resulted from only partial infilling of the conduits at the close of each earlier historical eruption and were subsequently enlarged by acid attack and erosion of the conduit walls. During the eruption these shallow voids were enlarged by continuous elutriation of lithic particles by the upward streaming of gas and vapour and by collapses, the largest of which produced visible surface changes, e.g. the 25 August 1977 events. The processes undermined the shallow fill in the western subcrater and led to catastrophic failures and the formation of Christmas and Gibrus craters. Christmas Crater formed because streaming of ash and gas through the new vent in advance of the rising magma (Fig. 21b) eroded and created instability of the fill beneath 1971 and 1933 craters. This area collapsed progressively but did not hinder continued advance of the magma through a conduit on the western margin of the new crater (Fig. 21c, d). By February 1978, the volume of erupted tephra equalled that of Christmas Crater, but the crater dimensions were unchanged, suggesting that the continued eruption of magma and country rock in 1977 had led to formation of more void space around the conduits. A major contributor was the large phreatomagmatic eruption on 25 August 1977 (Fig. 21f). Sufficient erosion had occurred by February 1978 to open the previously blocked conduit below Gilliver Crater (Fig. 21g). Once this happened, rapid removal of crater fill into the eruption columns (Fig. 4b) and collapse formed Gibrus Crater, at the expense of void space beneath Gilliver, Sulphur and Christmas craters. This collapse led to permanent blockage of the Gibrus conduits, and renewed volcanism took place from the western portion of Christmas Crater (Fig. 21h).

Nature of magma-to-water interaction

Eruptive mechanisms during the mild, near-continuous phreatic and phreatomagmatic eruptions were quite different from those of the larger, discrete, explosive events. The near-continuous emission of gas and mixed lithic and juvenile ash was characteristic of much of the eruption sequence. Gas streaming from the magma frittered juvenile clasts from the upper surface of the magma body and scoured lithic particles from the unconsolidated conduit walls (Fig. 22). Removal of the lithic particles was probably aided by expansion of adjacent pore fluid, and the clasts were carried upwards into a weakly convecting plume. The commonly observed pulsating nature of the emission was probably related to a cyclicity in the magmatic degassing, which is a common feature of Strombolian volcanoes. The frequency of the phreatomagmatic pulses and the emission velocities at White Island are similar to those observed during classical dry Strombolian eruptions (Blackburn et al. 1976). Fumarole temperatures at White Island prior to the 1976–1982 eruptions suggest that much of the groundwater involved in these events was already heated to temperatures on or close to the boiling-point-for-depth curve prior to incorporation in the eruption column. Very large quantities of extra heat were not required to vaporise this water, so that the mild, near-continuous phreatomagmatic eruptions made very efficient use of the limited quantity of heat supplied by the magmatic volatiles. The fine grain size of the deposits does not reflect efficient fragmentation; in fact, very little fragmentation probably occurred. Rather it is due to the pre-existing fine grain size of parts of the crater fill, which were preferentially eroded, and to their weak, hydrothermally altered state. Multiple recycling of tephra through the vent was also a contributing factor. Tephra was recycled both by fallback during eruption and by slumping and sheet erosion of proximal tephra back into the collapse craters.

These weak, near-continuous phreatic to phreatomagmatic eruptions at White Island were a long-term, sustained process involving magma only rather passively. The larger discrete explosions were quite different and caused by brief, violent, direct contact of magma and shallow groundwater. The key features of the large discrete phreatomagmatic explosions were:

1. The shallow focus, i.e. within the loose fill of the western subcraters
2. The thermal heterogeneity of the ejecta
3. The random occurrence of the events and lack of discernible precursors
4. The strong link to collapse crater formation

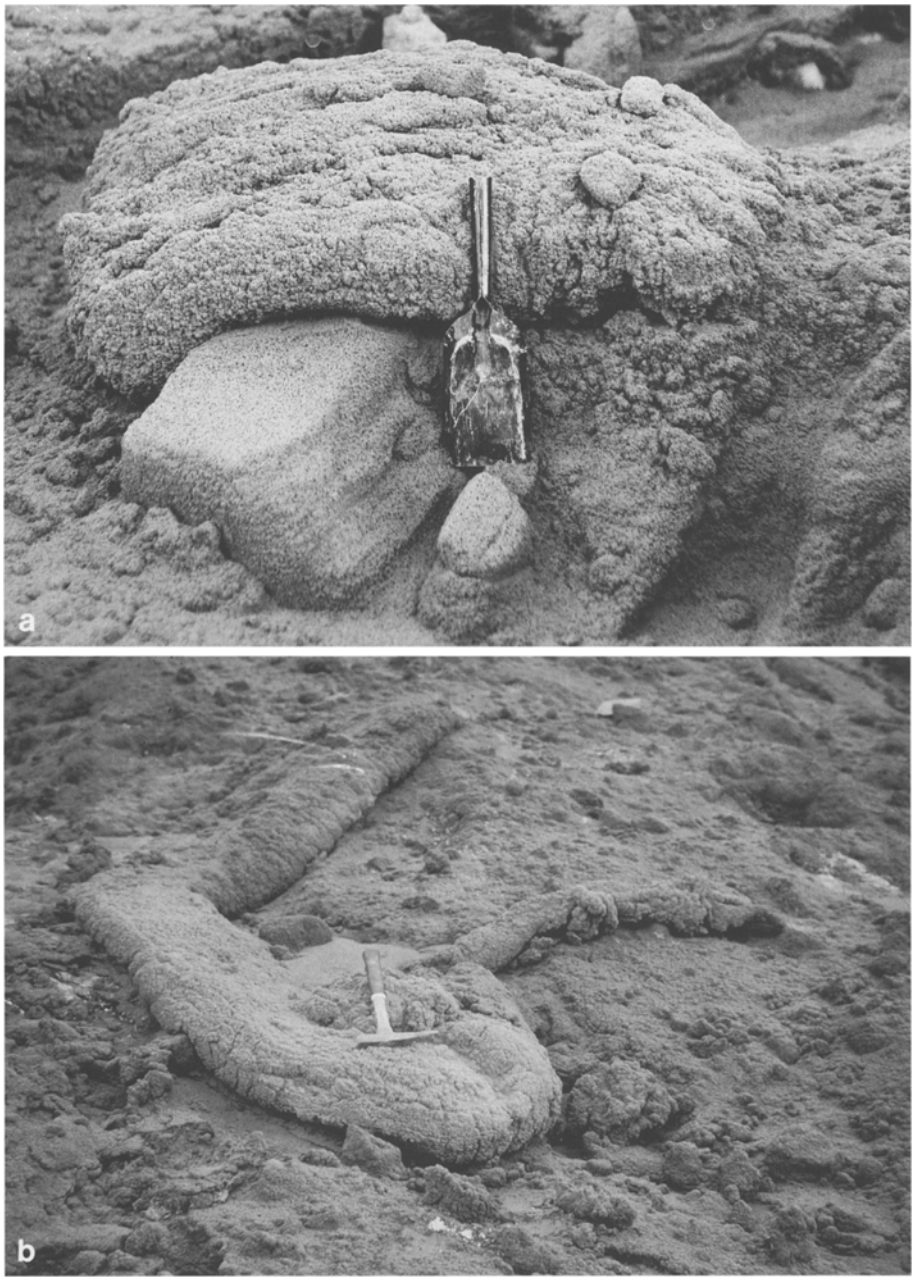

Fig. 18. a Compact fluid bomb with breadcrusted surface. Scale is 430 mm. S1 phase, 4 April 1977. Photograph by IA Nairn. **b** 4-m ribbon bomb 350 m from vent. S1 phase, 4 April 1977. Photograph by S. Nathan

5. The extended quiescence following the larger phreatomagmatic eruptions

We believe the large discrete phreatomagmatic eruptions were triggered by sudden contact of magma and saturated country rock during collapse of the conduit walls beneath the vents. The large, discrete phreatomagmatic explosions all took place well after the S1 peak of magma advance, at times when magma appears to have been retreating from the vent system, and this was a further contribution to instability of the conduits. In our model, sudden collapse of conduit walls triggered explosive eruption, and promoted partial mixing of wet wall rock and magma. It is impossible to assign a unique magma-to-water ratio for such heterogeneous events. The eruption assemblage had four components: magma, gas, wall rock and groundwater. Each component was itself heterogeneous. The magma was generally derived from the quenched margin of the magma body, which was thermally stratified and partially degassed to varying degrees. Occasionally, hotter actively degassing magma also was involved. The magmatic gas component consisted of both steam and noncondensable gases. The country rock had widely ranging pre-existing grain size and was at temperatures extending from ambient to gas-heated incandescence adjacent to the active conduits. The groundwater component ranged from cold meteoric runoff, through acidic heated brine, to brine/vapour mixtures. There was little opportunity for mixing and homogenisation of these diverse components during eruption and no single mag-

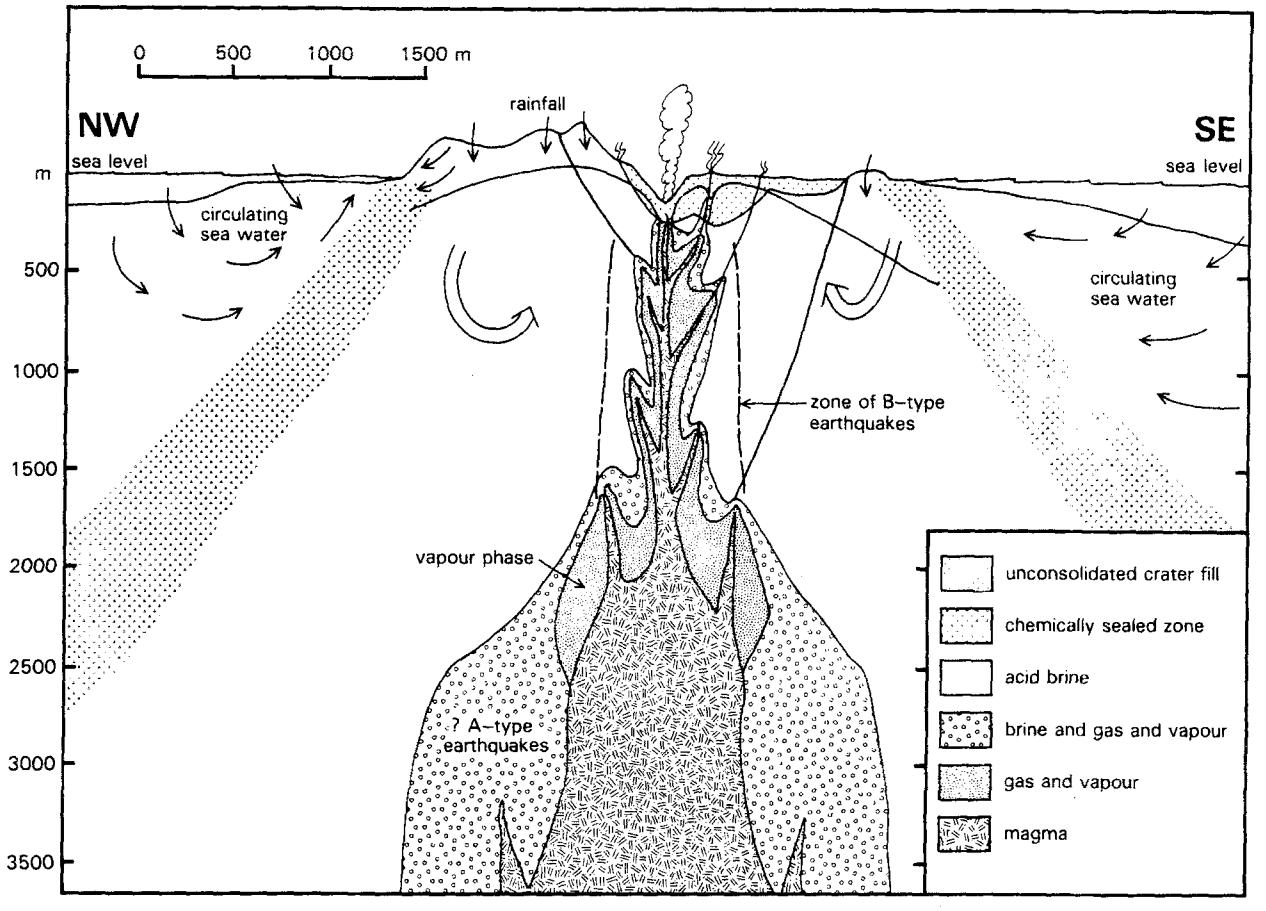

Fig. 19. Cartoon of the subsurface structure and hydrology of White Island volcano, inferred from structural, seismic and chemical data

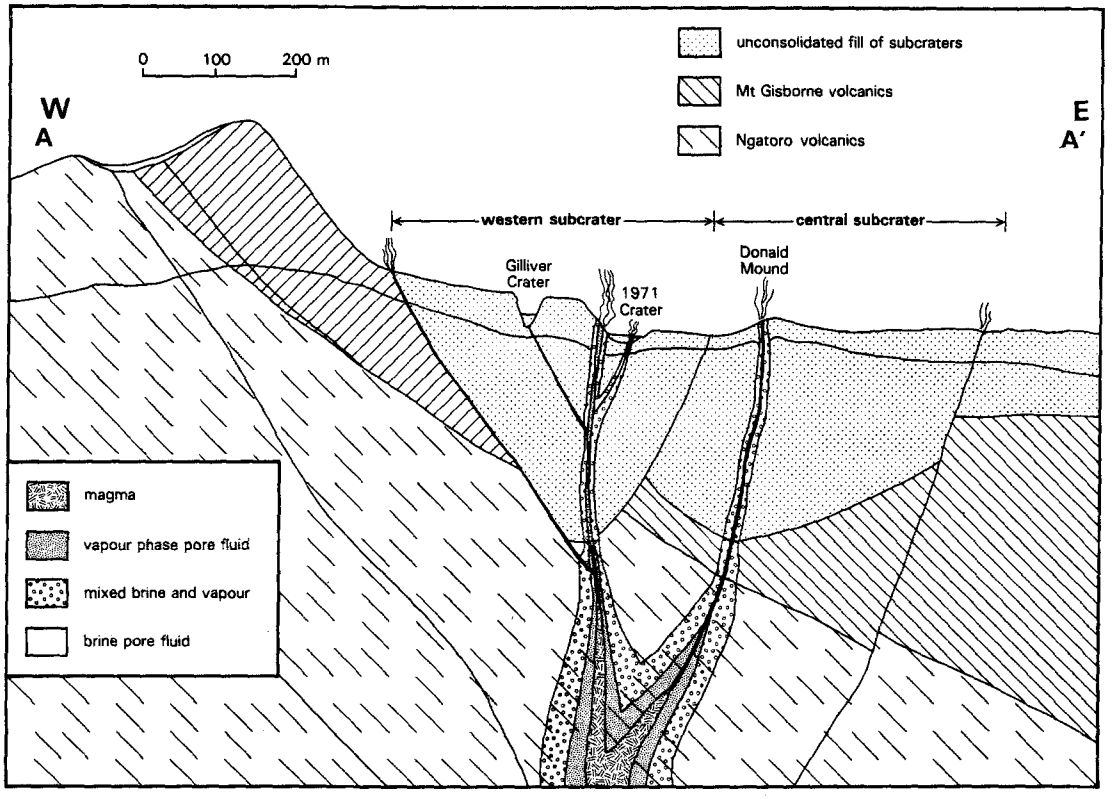

Fig. 20. Schematic section through the White Island vents in December 1976 immediately prior to the onset of the eruption sequence. Envelopes of vapour and hot brine enclose conduits leading to 1971 Crater and Donald Mound, but magma has been preferentially channeled towards 1971 Crater

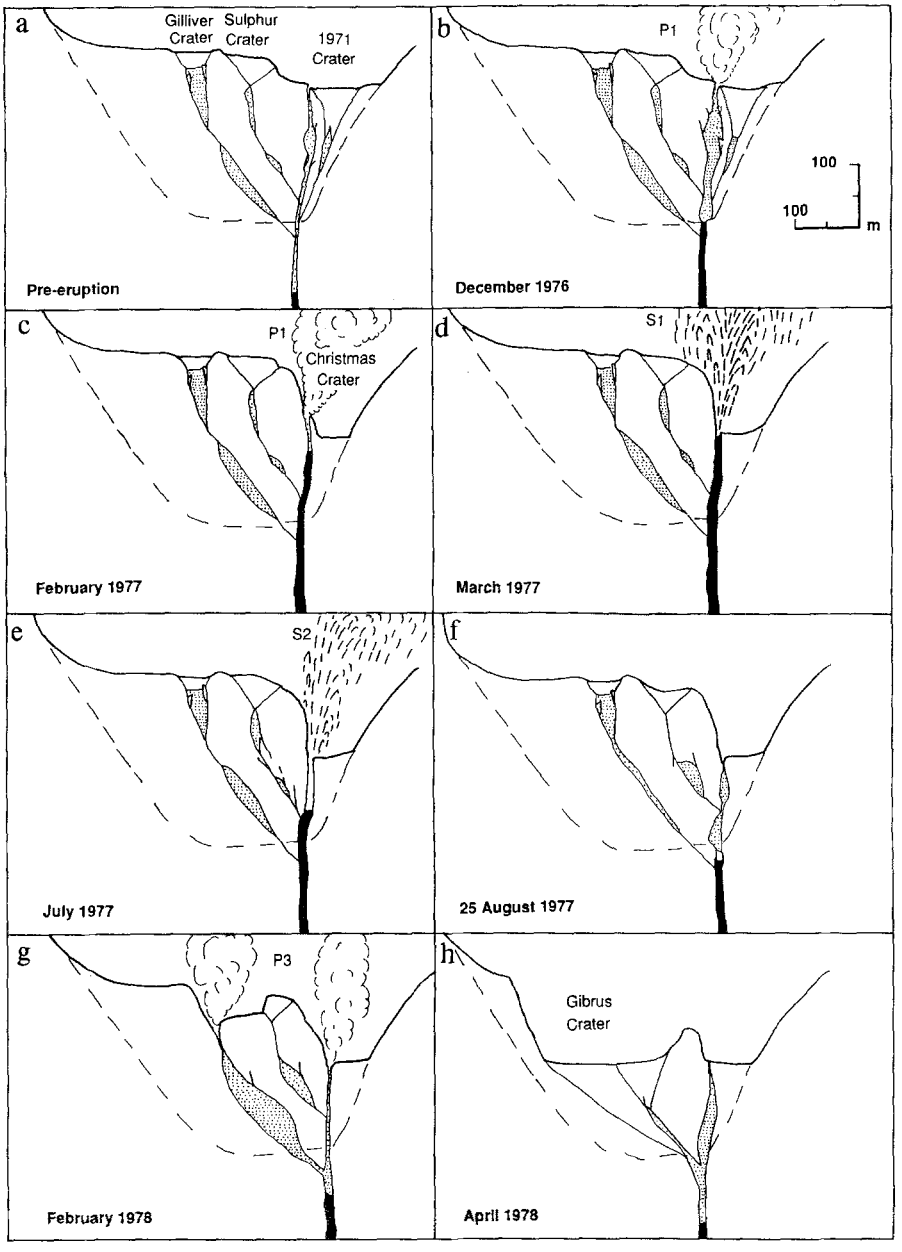

Fig. 21a–h. Cross-sections showing crater development during the 1976–1982 eruption at White Island. *Stippled* areas represent subsurface voids developed along conduits. (See text for details.)

ma-to-water ratio is applicable to all parts of the material ejected in each phreatomagmatic explosion.

Model for the eruption sequence

Degassing of rising andesite magma, and heating and local evaporation of the saline acidic groundwater led in 1976 to increased flow of gas and vapour through the partially blocked conduits beneath Donald Mound and 1971 Crater. Eruptions began in December 1976 when the flow rates of the escaping gas/vapour phase were sufficiently high to strip ash from the poorly consolidated crater-fill forming the conduit walls. This removal of material from above the advancing magma caused small-scale subterranean collapse and formation of a saucer-shaped surface depression, which grew rapidly into the steep-walled, collapse-dominated Christmas Crater. As magma reached depths of less than 100 m, increasing volumes of ash were frittered from the quenched/degassed margin of the magma body, so that the juvenile content of the ash deposits increased rapidly in February 1977. Magma advance and wall erosion continued until actively vesiculating magma was first exposed in March 1977 and Strombolian volcanism ensued. This first Strombolian phase (S1) occurred at the highest level reached by the magma during the eruption, and slow retreat of the main body then occurred from March 1977 onwards. As the rate of magma supply decreased, degassed magma ponded in the vent, leading to only mildly explosive degassing, and ultimately to the close of Strombolian volcanism. The continued flux of gas and vapour led to a resumption of phreatomagmatic volcanism (P2), which included some larger discrete explosions when portions of the conduit walls collapsed, temporarily blocking the

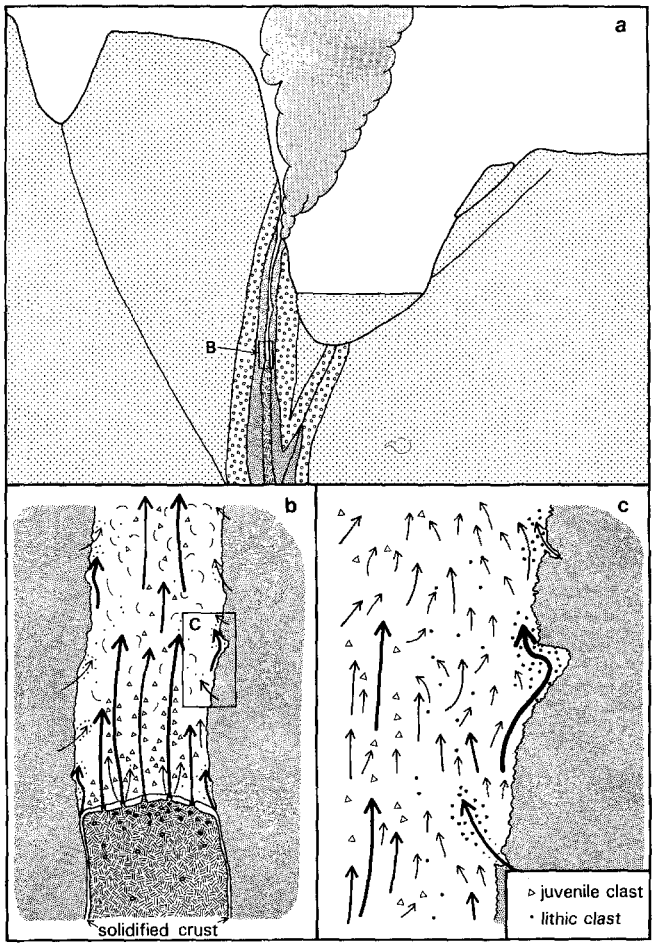

Fig. 22a–c. Model for the near-continuous phreatomagmatic eruptions on White Island. Magmatic volatiles and steam strip juvenile clasts from the degassed crust (*white*) of the magma body and stream up the conduit eroding ash from the vapour-saturated conduit walls (*stippled*)

vent. A second phase of open-vent Strombolian eruption (S2) began when actively vesiculating magma was again exposed in late July 1977, but at considerably greater depth than during the S1 event. This activity had declined to weakly explosive degassing again by 25 August 1977, when a major collapse occurred in the complex conduit system beneath the pre-1976 vents, triggering the large phreatomagmatic eruption. The P3 phreatomagmatic phase continued with a series of similar events, and vent position changed frequently as a result of temporary blockage and clearance of portions of the complex system of pre-existing shallow conduits. Widespread instability and collapse following the clearance of the conduit beneath Gilliver Crater culminated in the formation of Gibrus Crater and the large explosive eruptions of March 1978. An extended repose period followed, as the shallow conduit system had been extensively modified by the Gibrus collapse, but a resumed flow of gas and vapour led to mild, near-continuous phreatomagmatic eruption and ultimately the S3 Strombolian phase between February 1979 and November 1980. The great depth of the fragmentation surface at this time precluded formation of thick scoria fall deposits on the main crater floor, and ultimately the supply of actively vesiculating magma declined. Phreatomagmatic volcanism resumed, but much of the ejecta fell back into 1978 Crater Complex and was recycled. By 1982 the reduced vigour of degassing and declining level of magma-to-water interaction could no longer counteract blockage of the conduit by wall collapse and the fallback of ejecta, and the eruption sequence ended.

Conclusions

The outstanding features of the 1976–1982 White Island eruption sequence were the low discharge rate of magma over an extended time period and the unusual physical setting, in which magma and magmatic volatiles interacted with abundant but finite quantities of groundwater in a confined hydrothermal system. Other influences on the 1976–1982 eruption sequence were: (1) the fine-grained and brine-saturated, unconsolidated nature of the conduit wall material, and (2) the location of partially blocked pre-existing conduits in the vent area.

A key factor not previously recorded for phreatomagmatic eruptions is that the flux of magmatic volatiles was consistently significant at White Island even during phreatic phases and remained high during the repose period after 1982 (Rose et al. 1986). The rise rate of magma was so low that gas was discharged by continuous streaming through the shallow magma, as well as during eruptions of actively vesiculating magma.

The pre-existing conduits active in 1933–1971 were important as channelways for both magma and decoupled magmatic volatiles, but also served as foci for development of the subterranean voids, which permitted sudden crater collapse. The long duration of the near-continuous phreatomagmatic eruptions was only possible because of finite quantities of 'pre-heated' groundwater in the conduit walls. The high enthalpy of this fluid meant that little additional heat was required from the magma to produce rapid vaporization and expansion of the pore fluid. The low strength and instability of the crater-fill material comprising the conduit walls were key features in determining the course of phreatomagmatic phases of the eruption. While the conduit walls remained stable, the loose ash was quickly and efficiently removed by the streaming of gas and vapour in the near-continuous phreatomagmatic eruptions, but this erosion was itself a contributing factor in producing conduit-wall instability and collapse, generating the larger discrete phreatomagmatic explosions.

The course of the eruption sequence was thus controlled by delicate balances of: (1) the rates of magma rise and discharge and gas discharge rates and (2) conduit-wall erosion versus conduit-wall collapse. The White Island eruptions represent a very complex interaction at shallow levels between four heterogeneous components of the volcano: a long-lived hydrothermal system, prehistoric craters filled with weak, unconsolidated fill, rising basic magma, and a sustained flux of

magmatic gas. In this system, hydrological factors were as important as magmatic ones in determining the form of the eruptions, and the ubiquitous role of exsolved magmatic volatiles obscured the distinction between 'phreatic' and 'phreatomagmatic' phases of the volcanism.

Acknowledgements. We wish to acknowledgement the efforts of many colleagues who have contributed to the White Island project, but especially R. H. Clark, J. W. Cole, W. F. Giggenbach, P. M. Otway and B. J. Scott. J. R. Buttle allowed access to his private volcano, and RNZAF No. 3 Squadron supplied helicopter transport and personnel to assist with work on the island. Peter Kokelaar, Dan Miller, and Colin Wilson contributed detailed reviews, and we greatly appreciated Ulrich Bednarz's thoughtful review of the final manuscript.

References

Black PM (1970) Observations on White Island Volcano, New Zealand. Bull Volcanol 34:158–167

Blackburn EA, Wilson L, Sparks RSJ (1976) Mechanisms and dynamics of strombolian activity. J Geol Soc Lond 132:429–440

Christoffel DA (1989) Variations in magnetic field intensity at White Island volcano related to the 1976–82 eruption sequence. NZ Geol Surv Bull 103:109–118

Clark RH, Otway PM (1989) Deformation monitoring associated with the 1976–82 White Island eruption sequence. NZ Geol Surv Bull 103:69–84

Cole JW, Nairn IA (1975) Catalogue of the active volcanoes of the world including Solfatara fields. Part 22: New Zealand. International Association of Volcanology and Chemistry of the Earth's Interior, Naples

Duncan AR (1970) Eastern Bay of Plenty volcanoes. Unpublished PhD thesis lodged in the Library, Victoria University of Wellington

Fournier RO (1987) Conceptual models of brine evolution in magmatic-hydrothermal systems. In: Decker RW, Wright TL, Stauffer PH (eds) Volcanism in Hawaii. US Geol Surv Prof Paper 1350:1487–1506

Giggenbach WF (1987) Redox processes governing the chemistry of fumarolic gas discharges from White Island, New Zealand. Appl Geochem 2:143–161

Giggenbach WF, Glasby CP (1977) The influence of thermal activity on the trace metal distribution in marine sediments around White Island, New Zealand. NZ Dep Sci Ind Res Bull 218:121–126

Giggenbach WF, Sheppard DS (1989) Variations in the temperature and chemistry of White Island fumarole discharges 1972–85. NZ Geol Surv Bull 103:119–126

Healy J (1968) Aerial inspection of White Island, 21 February 1968. Unpublished report on open file. NZ Geological Survey, Rotorua

Houghton BF, Nairn IA (eds) (1989a) The 1976–82 eruption sequence at White Island volcano, Bay of Plenty, New Zealand. NZ Geol Surv Bull 103:1–136

Houghton BF, Nairn IA (1989b) The phreatomagmatic and Strombolian eruption events at White Island volcano 1976–82: eruption narrative. NZ Geol Surv Bull 103:13–23

Houghton BF, Nairn IA (1989c) A model for the 1976–82 phreatomagmatic and Strombolian eruption sequence at White Island volcano, New Zealand. NZ Geol Surv Bull 103:127–136

Houghton BF, Scott BJ, Nairn IA, Wood CP (1983) Cyclic variation in eruption products, White Island volcano, New Zealand 1976–1979. NZ J Geol Geophys 26:213–216

Houghton BF, Nairn IA, Scott BJ (1989) Phreatomagmatic and Strombolian eruptive activity at White Island volcano 1976–82: deposits and depositional mechanisms. NZ Geol Surv Bull 103:35–56

Jaupart C, Vergniolle S (1988) Laboratory models of Hawaiian and Strombolian eruptions. Nature 331:58–60

Martin RC (1959) White Island Activity. Unpublished report on open file. NZ Geological Survey, Rotorua

Murase T, McBirney AR (1973) Properties of some common igneous rocks and their melts at high temperatures. Geol Soc Am Bull 84:3563–3592

Nairn IA, Houghton BF (1989) Formation of collapse craters and morphological changes in the main crater of White Island volcano during the 1976–82 eruption sequence. NZ Geol Surv Bull 103:25–34

Rose WI, Chuan RL, Giggenbach WF, Kyle PR (1986) Rate of sulphur dioxide and particle emission from White Island volcano, New Zealand, and an estimate of the total flux of major gaseous species. Bull Volcanol 48:181–188

Tomasson J, Kristmannsdottir H (1972) High temperature alteration minerals and thermal brines, Reykjanes, Iceland. Contrib Mineral Petrol 36:123–134

Vergniolle S, Jaupart C (1986) Separated two phase flow and basaltic eruptions. J Geophys Res 91:12842–12860

Editorial responsibility: H-U Schmincke